

People's Democratic Republic of Algeria

Ministry of Higher Education and Scientific Research
Ibn Khaldoun University of Tiaret
Faculty of Applied Sciences
Department of Civil Engineering



Course Handout Advanced Soil Mechanics: Course and Exercises

Geotechnical Engineering

Dr: SERBAH Boumediene



Semester: 1
Credits: 4
Coefficient: 2
Copyright © 2026 Serbah b.h
boumediene.serbah@univ-tiaret.dz

Experts:
Pr. krim abdallah
Pr. TLIDJI youcef

First printing, January 2026

Contents

I Soil Mechanics Principles

I	Review of Coarse-Grained and Fine-Grained Soils	13
1.1	Introduction	13
1.2	Differences Between Coarse-Grained and Fine-Grained Soils	13
1.2.1	Coarse-grained soils	13
1.2.2	Behavior of Coarse-Grained Soils	13
1.2.3	Density Index or Relative Density	14
1.3	Properties of Fine-grained Soils	17
1.3.1	Structure of Fine-grained (clay):	17
1.3.2	Fine-grained (cohesive):	17
1.4	Plasticity and Shear Strength of Soils	19
1.4.1	Plasticity of Soils	22
1.5	Stresses, Strains, Elasticity, and Plasticity	23
1.5.1	Stress Tensor	23
1.5.2	Stress Distribution Around a Point	24
1.5.3	Normal and shear stresses on planes through a stress element	24
1.5.4	Consider a plane stress case:	24
1.5.5	Sign conventions for stresses	26
1.5.6	transformation of plane stress	26
1.5.7	Direct Calculation of Principal Stresses and Plane Orientation	28
1.5.8	Plane Representation – Mohr’s Circle	38
1.5.9	Two-Dimensional Problems	38
1.5.10	Shear Strength of Soils	39
1.5.11	Relationship Between Plasticity and Shear Strength	39
1.6	Linear Elasticity – Stress–Strain Relationships (Elastic Domain)	39
1.6.1	Basic Concepts of Elasticity (Review)	39
1.6.2	Equivalent Linear Elastic Behavior	40
1.6.3	Practical Considerations for Linear Elastic Representation of Soils	42

1.7	Stress Paths in (σ, ε) and (p, q) Spaces	42
1.7.1	Stress path in the (σ, ε) plane	42
1.7.2	Stress path in the (p, q) plane	42
2	Behavior of Fine-Grained Soils	43
2.1	Nature and Classification	43
2.2	Microstructure and Physico-Chemical Effects	43
2.3	Effective Stress and Pore Pressure	43
2.4	Compressibility and Consolidation	44
2.4.1	One-Dimensional Compression	44
2.4.2	Primary Consolidation	44
2.4.3	Secondary Compression (Creep)	44
2.5	Shear Strength of Fine-Grained Soils	44
2.5.1	Drained Strength	44
2.5.2	Undrained Strength	45
2.6	Stress History and Overconsolidation	45
2.7	Permeability and Hydraulic Conductivity	45
2.8	Shrink–Swell Behavior	46
2.9	Sensitivity and Structure	46
2.10	Laboratory and Field Testing	46
3	Behavior of Granular Materials	49
3.1	Dilatancy and Contractancy of Granular Media	49
3.2	Dilatancy Theory	49
3.3	Critical State and Characteristic State	49
3.4	Influence of Lateral Stress	50
3.5	Behavior under Cyclic Loading: Contraction, Dilation, and Liquefaction	50
4	Unsaturated Soil Behavior	53
4.1	Shrinkage and Swelling of Soils and Their Impact on Structures	53
4.1.1	Definition	53
4.2	Definition of Suction	53
4.2.1	Concept of Effective Stress in Unsaturated Soils	54
4.3	Water in Unsaturated Soils	54
4.3.1	Soil Water Components	54
4.3.2	Soil Moisture Characteristics	55
4.3.3	Movement of Water in Unsaturated Soils	55
4.3.4	Engineering Implications	55
4.3.5	Shear Strength of Unsaturated Soils	56
4.3.6	Permeability and Suction	56
4.4	Properties of Water in an Unsaturated Porous Medium	57
4.4.1	Surface Tension Force	57
4.4.2	Surface Tension and Pressure in a Bubble	58

4.5	Measurement of Surface Tension	58
4.5.1	Capillary Method	58
4.5.2	Tensile Force on a Submerged Plate	59
4.5.3	Wettability	60
4.5.4	Observations	60
4.5.5	Three Parameters Governing Contact Angle	60

List of Figures

1.1	Various types of sand exhibiting different colors	14
1.2	granular soil	15
1.3	Relative Density of Granular Soils	16
1.4	Structure of clay	18
1.5	Electron microscope images of clay	19
1.6	Soil cohesion results from molecular forces acting between adjacent particles	20
1.7	Fine-grained (cohesive)	20
1.8	Landslides :shear strength refers to the ability of soil to resist sliding along its internal layers	21
1.9	Geostatic stress due to soil self-weight and induced stress caused by foundation loading	21
1.10	soil plasticity and shear strength diagram	22
1.11	Soil plasticity and shear strength diagram	23
1.12	creep or plastic flow of the soil and its shear strength	23
1.13	Decomposed into a normal compressive stress σ_N and a shear stress τ .	24
1.14	The stress state described by the Cauchy stress tensor	25
1.15	Three-dimensional representation of the stress state at a point	25
1.16	Stress vector $T(M,n)$ at point M acting on an infinitesimal surface element dS	25
1.17	Direction of Stresses	26
1.18	the stress transformation relations	27
1.19		28
1.20	Direct shear test	32
1.21	Direct shear test: shear force versus normal force	34
1.22	three Mohr circles, $\sigma_1, \sigma_2, \sigma_3$	38
1.23	Field of Application: Linear Elasticity	40
1.24	Failure Criterion (Yield Criterion / Plasticity Law): Mohr–Coulomb, Drucker–Prager, von Mises	40
1.25	Overview of the Principal Aspects of Soil Behavior	41
1.26	Equivalent Linear Elastic Behavior	41
2.1	fine-grained soils (clay microstructure).	44
2.2	undrained shear strength	45

3.1	Dilatancy and Contractancy of Granular Media	50
3.2	Definition of the Characteristic State	51
3.3	Earthquake aftermath and ground subsidence	51
4.1	Shrinkage and Swelling of Soils and Their Impact on Structures	54
4.2	Concept of Effective Stress in Unsaturated Soils	55
4.3	Water in Unsaturated Soils	56
4.4	Permeability: Various Forms of Water in Unsaturated Soils	57
4.5	Analogy illustrating tensile forces: Forces acting on a slit created at the free surface of a liquid	57
4.6	Surface Tension and Pressure in a Bubble	59
4.7	Tensile Force on a Submerged Plate	59
4.8	the air-liquid interface	60
4.9	A drop of liquid	61
	
	
4.12	Representation of the capillary tub	63
4.13	Representation of the parameters of Laplace's law	63



List of Tables

1.1 Granular Soil Classification by Particle Size (Atterberg table) Followed by a geometric progression with a common ratio of $\frac{1}{10}$	14
1.2 Results of CD triaxial tests	37
2.1 Summary of CD triaxial test results	46
4.1 Contact angle values for different glass interfaces	61
4.2 Contact angle values for different interfaces	62



Soil Mechanics Principles

1	Review of Coarse-Grained and Fine-Grained Soils	13
1.1	Introduction	13
1.2	Differences Between Coarse-Grained and Fine-Grained Soils	13
1.3	Properties of Fine-grained Soils	17
1.4	Plasticity and Shear Strength of Soils	19
1.5	Stresses, Strains, Elasticity, and Plasticity	23
1.6	Linear Elasticity – Stress–Strain Relationships (Elastic Domain)	39
1.7	Stress Paths in (σ, ϵ) and (p, q) Spaces	42
2	Behavior of Fine-Grained Soils	43
2.1	Nature and Classification	43
2.2	Microstructure and Physico-Chemical Effects	43
2.3	Effective Stress and Pore Pressure	43
2.4	Compressibility and Consolidation	44
2.5	Shear Strength of Fine-Grained Soils	44
2.6	Stress History and Overconsolidation	45
2.7	Permeability and Hydraulic Conductivity	45
2.8	Shrink–Swell Behavior	46
2.9	Sensitivity and Structure	46
2.10	Laboratory and Field Testing	46
3	Behavior of Granular Materials	49
3.1	Dilatancy and Contractancy of Granular Media	49
3.2	Dilatancy Theory	49
3.3	Critical State and Characteristic State	49
3.4	Influence of Lateral Stress	50
3.5	Behavior under Cyclic Loading: Contraction, Dilation, and Liquefaction	50
4	Unsaturated Soil Behavior	53
4.1	Shrinkage and Swelling of Soils and Their Impact on Structures	53
4.2	Definition of Suction	53
4.3	Water in Unsaturated Soils	54
4.4	Properties of Water in an Unsaturated Porous Medium	57
4.5	Measurement of Surface Tension	58



1. Review of Coarse-Grained and Fine-Grained Soils

1.1 Introduction

Soil is a heterogeneous material composed of particles or crystals whose properties vary widely in terms of size, shape, and physicochemical behavior. Difference between coarse-grained soils and fine-grained. Cohesive behavior is exhibited by the soil when soil particles are very small and soil behavior is largely controlled by intergranular attraction forces, including electrical forces and Van der Waals forces.

1.2 Differences Between Coarse-Grained and Fine-Grained Soils

1.2.1 Coarse-grained soils

More than 50% of particles are larger than 0.08 mm (retained on sieve to 200 such as gravel, sand.). Soil without cohesion. their Behavior is governed by the properties of the solid skeleton and is little affected by water. In reality, soils are often composed of a mixture of particles of different sizes, (Figure 1.1) representing an intermediate state between coarse-grained and fine-grained soils.

1.2.2 Behavior of Coarse-Grained Soils

Behavior is governed by the properties of the solid skeleton and is **little affected by water**. In reality, soils are composed of a **mixture of particles of different sizes**, representing an **intermediate state between coarse-grained and fine-grained soils**.

- **Frictional forces between particles:**
 - Depend on particle shape, angularity, and packing density
 - Independent of water content
- **Shear strength:**
 - No tensile strength
 - Permeable

Table 1.1: Granular Soil Classification by Particle Size (Atterberg table)
 Followed by a geometric progression with a common ratio of $\frac{1}{10}$.

Type	Particle Size (D)
Rock blocks	$D > 200$ mm
Cobbles	$20 \text{ mm} < D < 200$ mm
Gravel	$2 \text{ mm} < D < 20$ mm
Coarse sand	$0.2 \text{ mm} < D < 2$ mm
Fine sand	$20 \mu\text{m} < D < 0.2$ mm
Silt	$2 \mu\text{m} < D < 20 \mu\text{m}$
Clay	$0.2 \mu\text{m} < D < 2 \mu\text{m}$
Ultra-fine clay	Less than $0.2 \mu\text{m}$



Figure 1.1: Various types of sand exhibiting different colors

1.2.3 Density Index or Relative Density

Relative density, also known as the density index, is a key parameter in geotechnical engineering used to describe the compactness state of coarse-grained or granular soils with respect to their extreme conditions. It quantifies the position of a soil in its natural state relative to its loosest configuration, characterized by the maximum void ratio, where soil particles are as far apart as possible while still maintaining contact, and its densest configuration, characterized by the minimum void ratio, where particles are packed as closely as possible without crushing. Consequently, relative density is defined based on the comparison between the in-situ void ratio and the limiting void ratios of the soil. This normalized measure provides a consistent basis for assessing the mechanical behavior of granular soils, including shear strength, stiffness, and compressibility, and it is widely used by geotechnical engineers to classify soils as very loose, loose, medium dense, dense, or very dense (figure 1.3).

To characterize the density state of a granular soil deposit (e.g., gravel or sand), one calculates its **density index** (I_D) or **relative density** (D_r) (figure 1.2). Density Index Formula = I_D . The density index (I_D) is calculated as:

$$I_D = \frac{e_{\max} - e}{e_{\max} - e_{\min}} \times 100 \tag{1.1}$$

where:

- e_{\min} : void ratio in the densest state;
- e_{\max} : void ratio in the loosest state;
- e : in-situ void ratio.

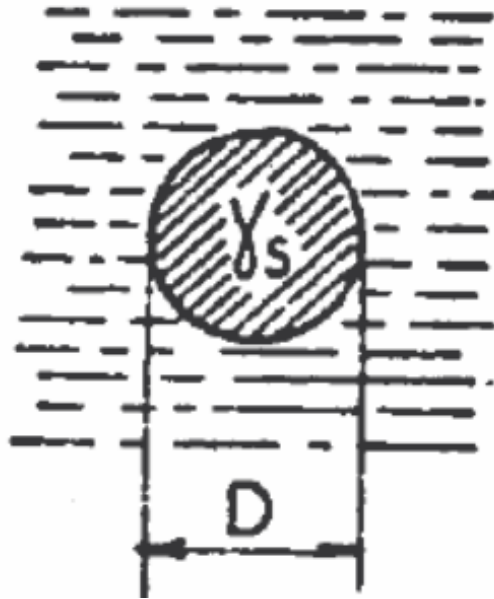
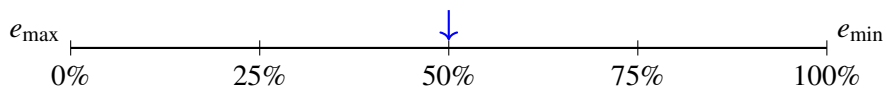


Figure 1.2: granular soil

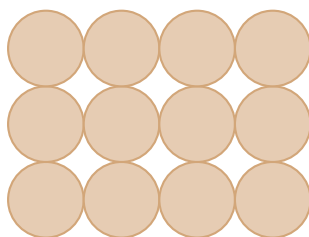
The density index (I_D) can be expressed in terms of void ratio (e) or dry density (ρ_d):

$$I_D(\%) = \frac{e_{\max} - e}{e_{\max} - e_{\min}} \times 100 = \frac{(\rho_d - \rho_{d,\min})}{(\rho_{d,\max} - \rho_{d,\min})} \cdot \frac{\rho_{d,\max}}{\rho_d} \times 100 \tag{1.2}$$

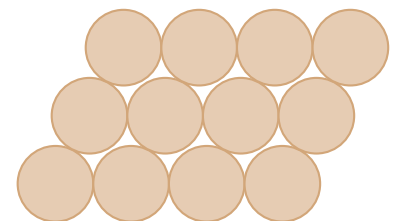
Void ratio scale:



Loosest Possible Configuration



Densest Possible Configuration



All soils in between
 →

D_r : This is a term used to indicate in-situ density state in comparison to loosest possible soil configuration ($D_r = 0\%$) and densest possible soil configuration ($D_r = 100\%$).

Relative density is only applicable to coarse-grained soils (i.e., sands and gravels). Not silts and clays. A lot of correlations are made with D_r including strength, settlement, permeability, etc. Typical natural soils seldom have $D_r < 20$ to 30%. Difficult to densify a soil in the field to $D_r > 85$

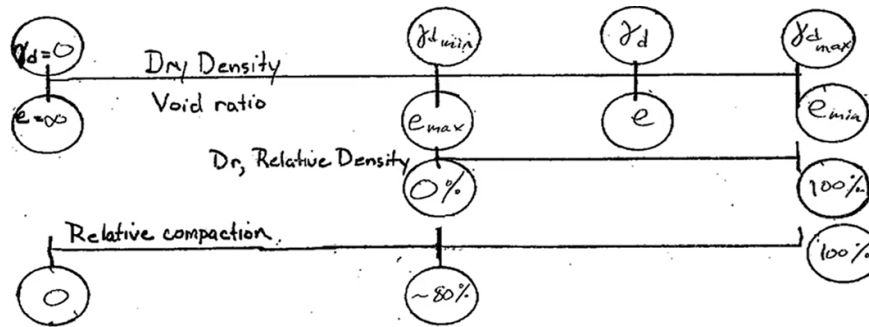


Figure 1.3: Relative Density of Granular Soils

Here are some commonly used descriptors of relative density among geotechnical engineers:

- Very Loose 0 - 15%
- Loose 15 - 35%
- Medium Dense 35 - 65%
- Dense 65 - 85%
- Very Dense 85 - 100%

Various geotechnical soil parameters are known to be influenced by relative density as ([friction angle](#) , [permeability](#), [liquefaction resistance](#) and [elastic modulus](#)).

Example (relative density)

A saturated sand layer along the Cooper River was found to have an in situ void ratio $e=0.7$. ASTM tests on the sand found it to have an $e_{max} = 0.85$ and $e_{min} = 0.4$. Assume $G_s=2.7$, answer the following questions

1. What is the in situ relative density D_r , of this sand deposit?
2. Based on the relative density chart, what would be the appropriate qualitative description of the firmness of this soil deposit?
3. Relatively speaking, would this be a good foundation material in its present state of firmness?
4. If the sand is compacted till $D_r=80$

(1) Determination of the in situ relative density

The in situ relative density D_r of the sand deposit is evaluated using the definition of relative density:

$$D_r = \frac{e_{max} - e}{e_{max} - e_{min}}$$

where:

$$e = 0.70, \quad e_{max} = 0.85, \quad e_{min} = 0.40$$

Substituting the given values:

$$D_r = \frac{0.85 - 0.70}{0.85 - 0.40} = \frac{0.15}{0.45} = 0.333$$

Therefore, the in situ relative density of the sand deposit is:

$$D_r \approx 33.3\%$$

(2) $D_r=33\%$ Loose

(3) Relatively speaking, the material cannot be considered a good foundation material in its present state of firmness.

(4) For $D_r=80\%$

$$D_r = \frac{e_{\max} - e}{e_{\max} - e_{\min}} * 100\% = 80\%$$

$$80\% = \frac{0.85 - e}{0.85 - 0.40} * 100\% = \frac{0.85 - e}{0.45} * 100\%$$

$e = 0.49$ (in situ void ratio after compaction)

$$\gamma_d = \frac{G_s \gamma_w}{1 + e} = \frac{2.7 * 10}{1 + 0.49} = 18 \text{ kN/m}^3$$

1.3 Properties of Fine-grained Soils

1.3.1 Structure of Fine-grained (clay):

More than 50% of particles are smaller than 0.08 mm (pass sieve to 200 such as silts and clay). Clay and silt soils with particle sizes below **20 μm** and exhibiting cohesion .

Their behavior changes markedly with water content, ranging from solid to plastic to liquid states (figure1.7).

Clay minerals strongly influence the engineering behavior of soils due to their unique microscopic structure.

Clay structure is formed from negatively charged hydroxyl ions and positively charged metallic cations, which naturally arrange themselves into fundamental polyhedral units known as silica tetrahedra and octahedra. These units link together by sharing hydroxyl ions to form extended silica and octahedral sheets.

The sheets subsequently stack through ionic (hydrogen) and covalent bonding, with the type of bonding depending on the availability of water and interlayer cations. Tightly bonded structures, such as kaolinite, are relatively inert, while minerals with weakly bonded or open interlayer spaces, such as montmorillonite, are highly reactive and capable of absorbing water and ions. As a result, the mineralogical structure of clays governs their reactivity, swelling behavior, and overall impact on soil engineering properties (figure1.4). Electron microscope images reveal that different clay minerals exhibit distinctly different microstructures, which strongly influence their engineering behavior. Some clays display jagged, plate-like particles with significant void space, while others, such as **kaolinite**, consist of uniform, tightly stacked sheets bonded by hydrogen bonds. In contrast, **montmorillonite** shows a highly open, honeycomb-like structure with abundant space for water and ions to enter, making it highly reactive. Many other clay minerals exist due to the numerous possible combinations of silica and octahedral sheets and interlayer cations, resulting in a wide range of mineralogies. Certain clays, such as **halloysite**, form tubular structures that can transform into kaolinite upon drying, while others like **vermiculite** present additional engineering challenges. In natural soils, clay minerals commonly occur as mixtures rather than in pure form, and familiarity with local clay mineralogy is therefore essential for geotechnical engineers.

1.3.2 Fine-grained (cohesive):

The behavior of fine-grained soil is a function of the mineral type and the moisture content.

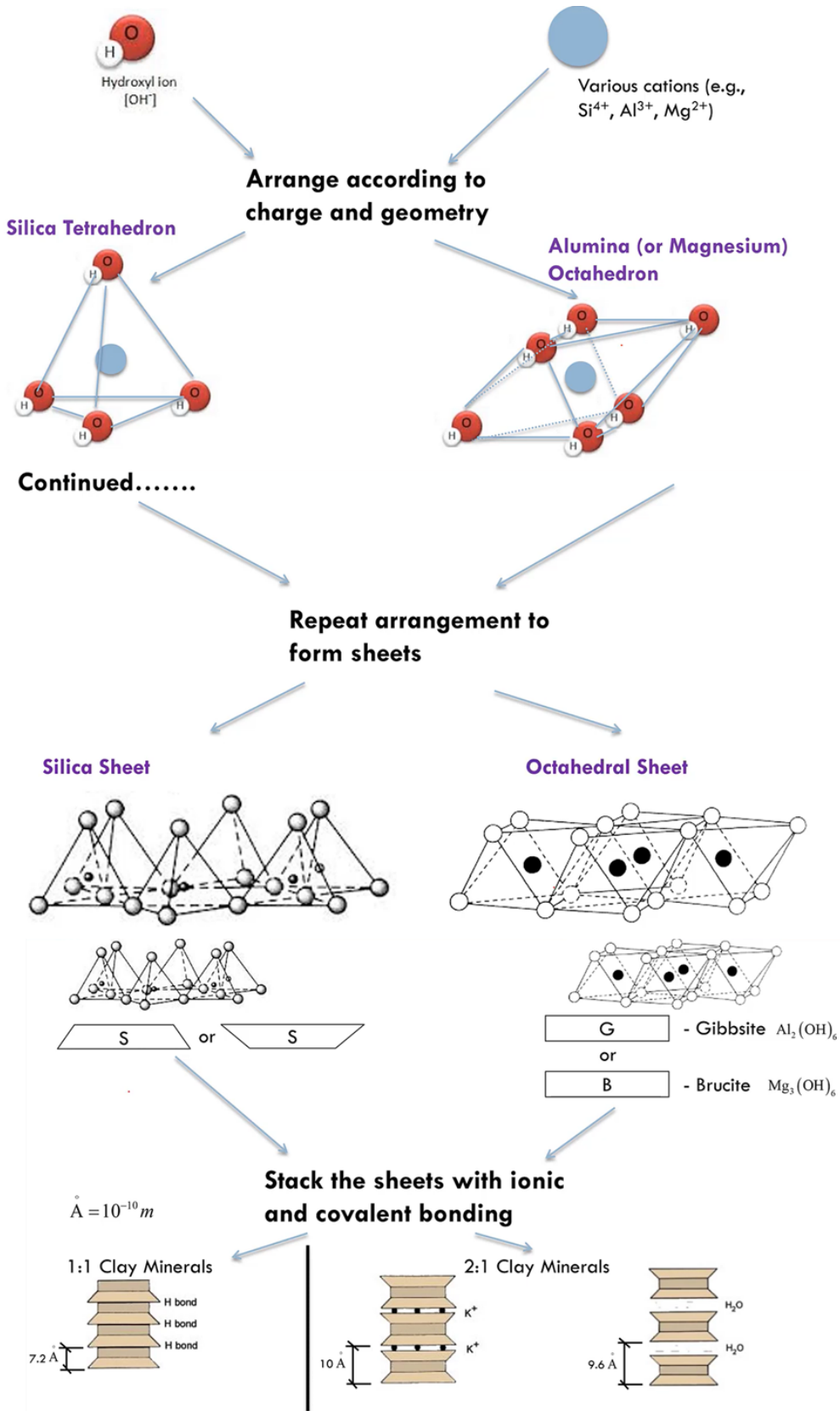


Figure 1.4: Structure of clay

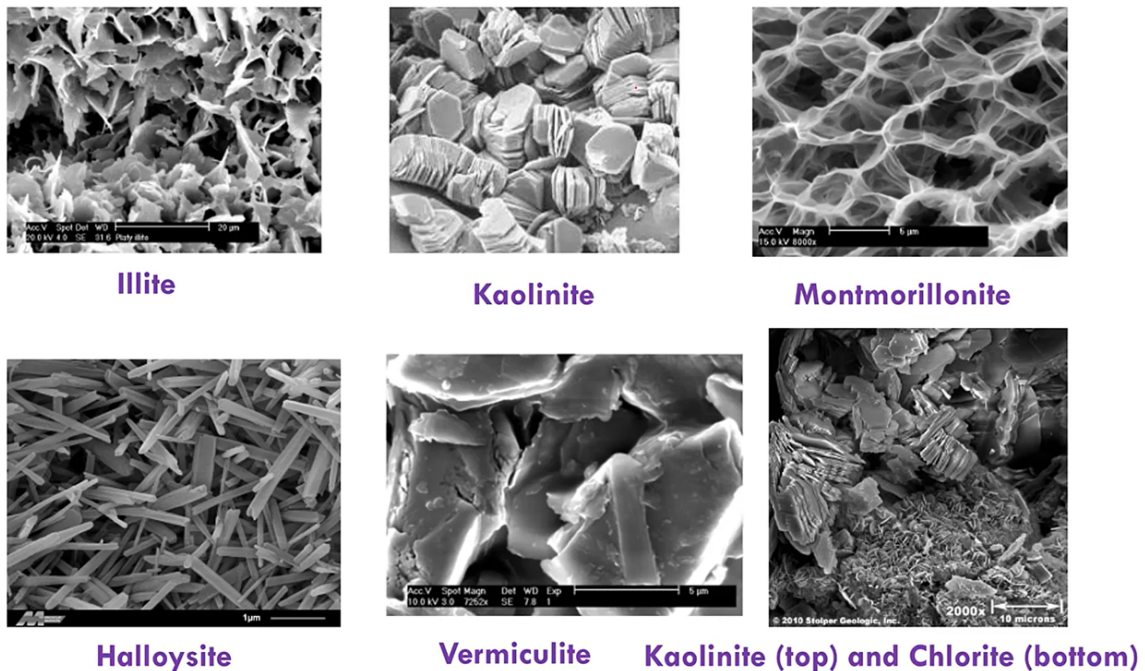


Figure 1.5: Electron microscope images of clay

This part, we are going to learn about why fine-grained soils behave the way that they do, and why water in particular makes them act a little whacky. Mineralogy is the primary factor controlling the size, shape, physical, and chemical properties of soil particles.

The Cohesion in fine-grained soils (i.e., clay and plastic silts) arises from **inter-particle friction and attraction forces**, which are influenced by:

- Particle shape and angularity , Very small particle size (i.e., $<2\mu\text{m}$).
- Packing density (compactness) and A relatively small amount of clay (e.g., $>10\%$ by weight) can significantly affect the properties of a soil mass as a whole!
- Surface characteristics
- Water content, Significant chemical interactions with one another, and with water and electrolytes.

Other key properties:

- Exhibits **shear and tensile strength**
- Generally **impermeable and frost-susceptible**
- **Water-sensitive**, prone to swelling and shrinkage

Soil cohesion results from molecular forces acting between adjacent particles. This figure 1.6 illustrates that the cohesion of clayey soils arises from molecular forces between adjacent particles. Such cohesion strongly influences soil behavior depending on water content.

1.4 Plasticity and Shear Strength of Soils

Landslides constitute a serious natural hazard that can occur unpredictably. What, then, causes these events, and why do they tend to occur more frequently during the rainy season? To answer these questions, it is essential to understand the concept of shear strength. In simple terms, shear strength refers to the ability of soil to resist sliding along its internal layers, figure 1.8.

Before examining the mechanisms that lead to landslides, it is essential to define and understand the concepts of total normal stress and shear stress acting within soil masses. Total normal stress refers to the force per unit area acting perpendicular to a given plane in the soil, whereas shear stress is the force acting parallel to that plane and is directly responsible for potential sliding. Landslides



Figure 1.6: Soil cohesion results from molecular forces acting between adjacent particles



The behavior of clayey soils is highly dependent on water content, making it a fundamental concern in geotechnical engineering.

Figure 1.7: Fine-grained (cohesive)

are hazardous phenomena that may occur suddenly, particularly during the rainy season, when soil shear strength defined as the ability of soil to resist sliding along its internal layers tends to decrease. For this reason, engineers and Master-1 students in Geotechnical Engineering, Structural Engineering, and Roads and Bridge Engineering must be able to distinguish between geostatic stresses, which naturally exist in the ground due to self weight, and induced stresses generated by external loads. Using analytical equations and Mohr's circle, the normal and shear stresses acting on planes of arbitrary orientation can be determined, along with the principal stresses and the orientation of the principal planes. In addition, the pole (or origin of planes) method provides an efficient graphical tool for determining stresses on planes with different orientations, thereby improving the assessment of stress conditions that may lead to soil failure and landslide initiation

Learning Objectives:

- Explain the differences between geostatic and induced stresses in the soil.
- Use Mohr's circle and/or equations to find :
 1. the principal stresses in a soil element
 2. the orientation of the principal planes
 3. the normal and shear stresses acting on any plane through a soil element.
- Stresses in a soil mass play a fundamental role in ensuring satisfactory ground performance , particularly when effective stress is properly considered. However, these stresses may



Figure 1.8: Landslides :shear strength refers to the ability of soil to resist sliding along its internal layers

become problematic when they result in excessive or undesirable deformations.

- In soil mechanics, stresses are commonly classified into two main categories.
 - 1- Geostatic stresses are those that arise solely from the self-weight of the soil and the presence of groundwater.
 - 2- In contrast, induced stresses are generated by external actions such as the construction of embankments, fills, foundations, and other engineering structures.

Understanding the distinction between geostatic and induced stresses is essential for analyzing soil behavior and predicting deformation and failure mechanisms.

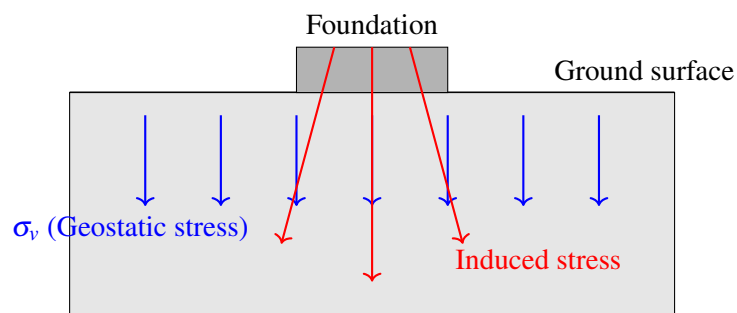


Figure 1.9: Geostatic stress due to soil self-weight and induced stress caused by foundation loading

In practice, solving a soil mechanics problem generally involves the following steps:

1. **Verify stability** — Check whether stability against failure is ensured with a satisfactory factor of safety.
2. **Check compatibility** — Ensure that the design of the structure is compatible with the allowable settlements.

In soils, **friction** corresponds to the resistance between one set of soil grains sliding over another.

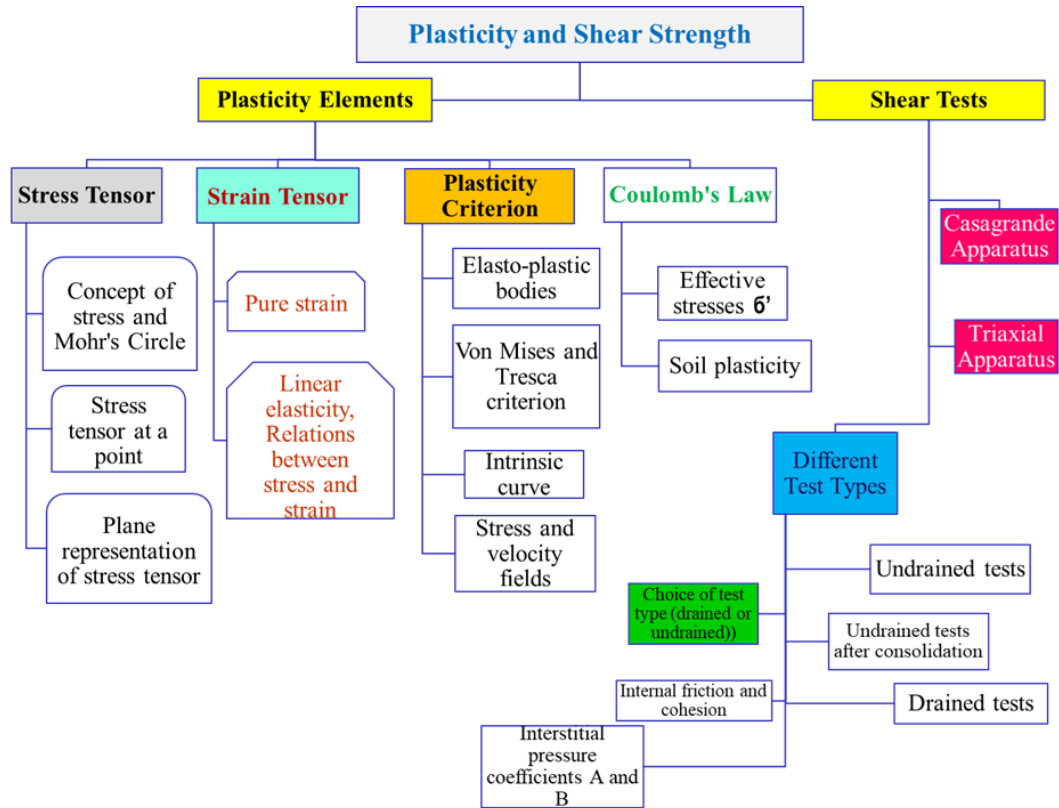


Figure 1.10: soil plasticity and shear strength diagram

1.4.1 Plasticity of Soils

Plasticity describes the ability of fine-grained soils, particularly clays, to undergo deformation without cracking or breaking when subjected to changes in water content.

As the water content increases, soil passes through four consistency states:

- **Solid state**
- **Semi-solid state**
- **Plastic state**
- **Liquid state**

The boundaries between these states are defined by the Atterberg limits:

- Shrinkage Limit (SL)
- Plastic Limit (PL)
- Liquid Limit (LL)

The plasticity index is defined as:

$$PI = LL - PL \quad (1.3)$$

A high plasticity index generally indicates a clayey soil with high compressibility and low permeability.

Plasticity and Shear Strength of Soils

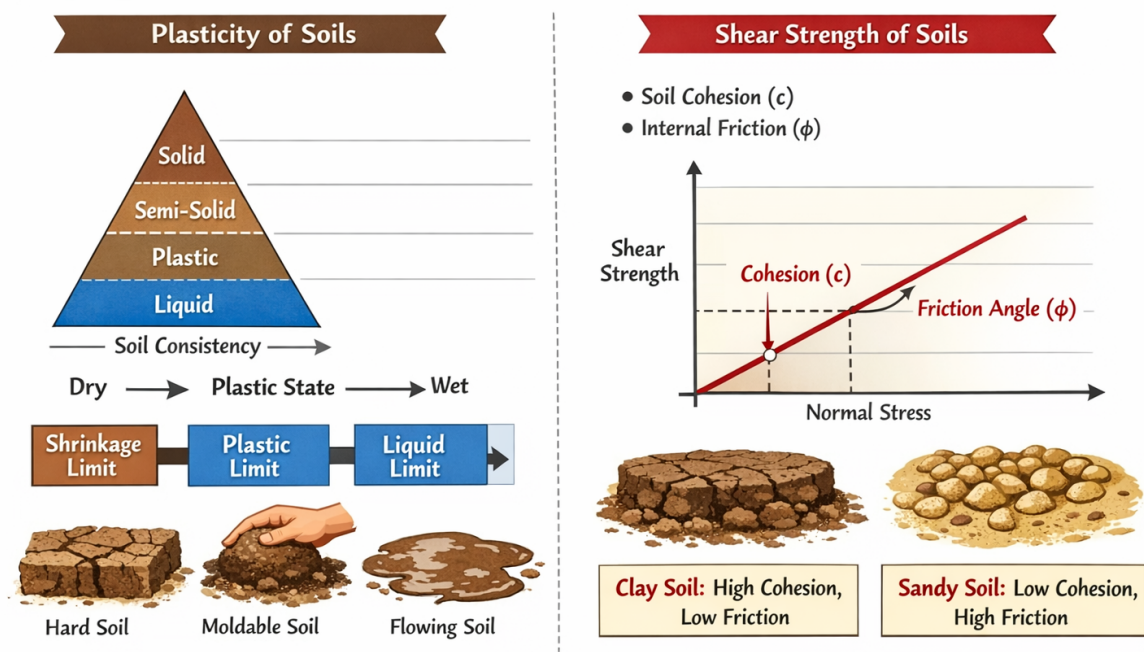


Figure 1.11: Soil plasticity and shear strength diagram

1.5 Stresses, Strains, Elasticity, and Plasticity

The behavior of soil under large increases in load, that is in the domain of large deformations and failure: creep or plastic flow of the soil, figure (1.10) and its shear strength. Shear strength is defined as the maximum shear stress that the soil can withstand, figure (1.12).

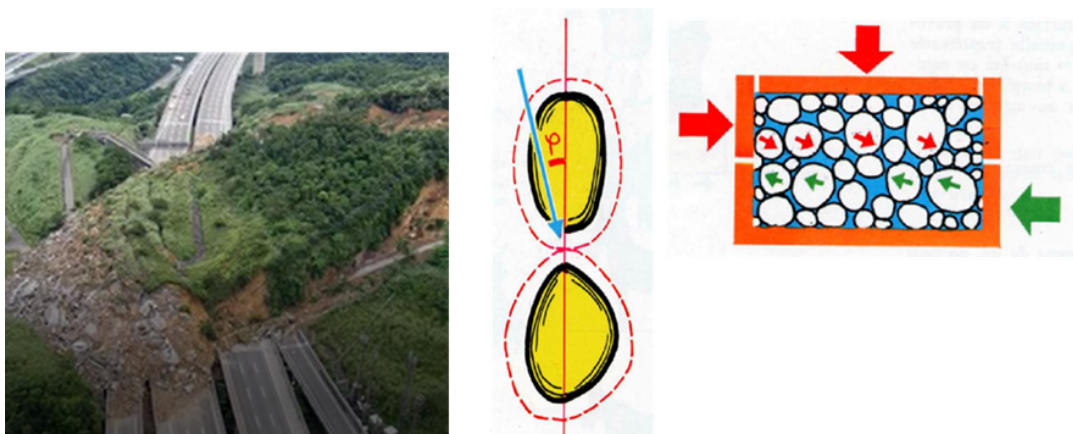


Figure 1.12: creep or plastic flow of the soil and its shear strength

1.5.1 Stress Tensor

Considering a soil element, it can be subjected to an arbitrary total stress σ_t , which can be decomposed into a normal compressive stress σ_n and a shear stress τ . This decomposition is

fundamental for analyzing the stress state within the soil, figure 1.13, as it allows the characterization of both volumetric compression and shear deformation, which are critical for understanding soil behavior under loading conditions. The most general state of stress at a point may be represented

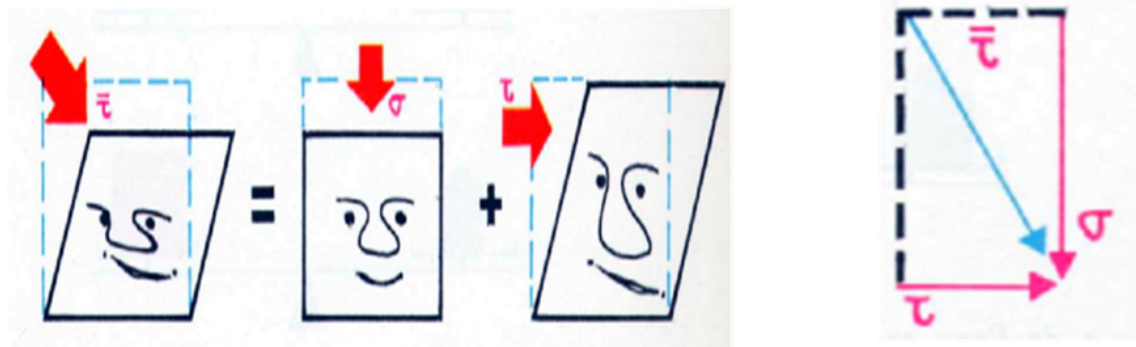


Figure 1.13: Decomposed into a normal compressive stress σ_N and a shear stress τ .

by 6 components, (figure 1.15):

- $\sigma_x, \sigma_y, \sigma_z$ normal stresses
- $\tau_{xy}, \tau_{yz}, \tau_{zx}$ shearing stresses

(Note: $\tau_{xy} = \tau_{yx}, \tau_{yz} = \tau_{zy}, \tau_{zx} = \tau_{xz}$) Same state of stress is represented by a different set of components if axes are rotated, figure 1.22

1.5.2 Stress Distribution Around a Point

The stress state at a point can be represented in three dimensions by an infinitesimal cubic element subjected to normal and shear stresses acting on its faces 1.15. When the cube is oriented along the Cartesian axes $x, y,$ and $z,$ the stress state at the point is described by the Cauchy stress tensor:

$$\sigma = \begin{bmatrix} \sigma_x & \tau_{xy} & \tau_{xz} \\ \tau_{yx} & \sigma_y & \tau_{yz} \\ \tau_{zx} & \tau_{zy} & \sigma_z \end{bmatrix} \quad \text{and} \quad \sigma' = \begin{bmatrix} \sigma'_x & \tau'_{xy} & \tau'_{xz} \\ \tau'_{yx} & \sigma'_y & \tau'_{yz} \\ \tau'_{zx} & \tau'_{zy} & \sigma'_z \end{bmatrix}$$

or equivalently into the primary constraint basis:

$$\sigma = \begin{bmatrix} \sigma_{11} & 0 & 0 \\ 0 & \sigma_{22} & 0 \\ 0 & 0 & \sigma_{33} \end{bmatrix}$$

1.5.3 Normal and shear stresses on planes through a stress element

The normal stresses ($\sigma_x, \sigma_y, \sigma_z$) act perpendicular to the faces of the cubic element, while the shear stresses ($\tau_{xy}, \tau_{xz}, \tau_{yz}$) act tangentially to these faces. This three-dimensional representation is fundamental in continuum mechanics and soil mechanics, as it allows a complete description of the stress state at a point, which is essential for analyzing deformation and failure mechanisms in soils 1.22.

1.5.4 Consider a plane stress case:

- σ_x normal stress in x -direction
- σ_y normal stress in y -direction
- τ_{xy} shear stress on **face** perpendicular to x -axis

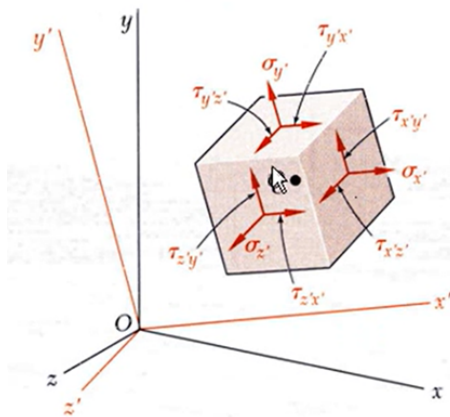


Figure 1.14: The stress state described by the Cauchy stress tensor

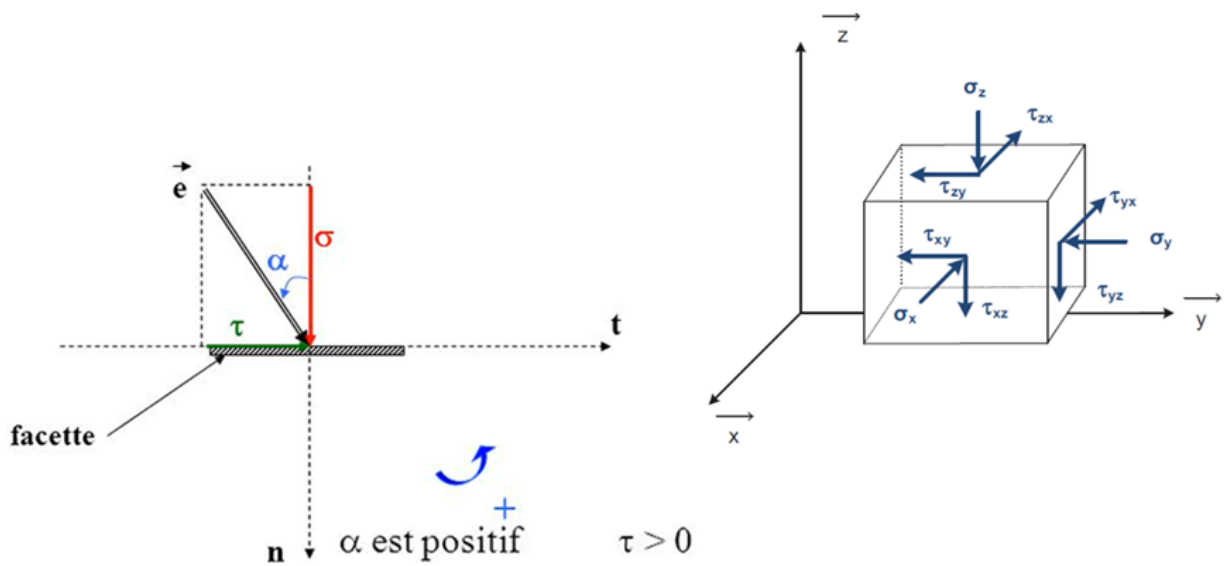


Figure 1.15: Three-dimensional representation of the stress state at a point

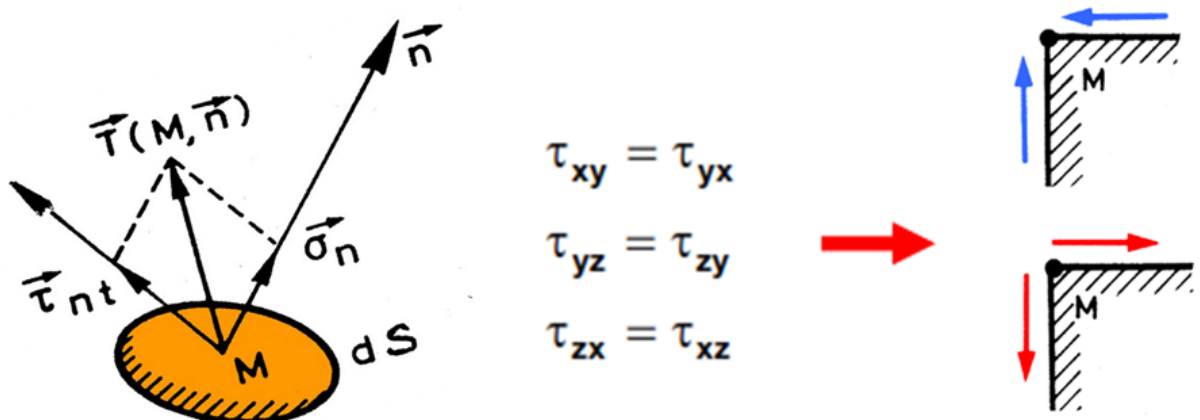


Figure 1.16: Stress vector $T(M,n)$ at point M acting on an infinitesimal surface element dS

in y-axis direction.

τ_{xy} is on vertical plane, τ_{yx} is on horizontal plane

Among the infinite number of planes passing through a point M , there exist three mutually

orthogonal **privileged planes** on which the **shear stress is zero** ($\tau = 0$). These planes are referred to as the **principal planes**, and their orientations define the **principal directions**. The normal stresses acting on these planes are called the **principal stresses**, denoted as:

- σ_1 : major principal stress,
- σ_2 : intermediate principal stress,
- σ_3 : minor principal stress,

with the ordering:

$$\sigma_1 \geq \sigma_2 \geq \sigma_3.$$

In soil mechanics, compressive stresses are conventionally taken as positive, and the normal to a plane is assumed to be oriented inward toward the element, in contrast to the outward normal convention commonly adopted in solid mechanics. This sign convention, together with the concept of principal stresses, enables a simplified and physically meaningful characterization of the stress state at a point, facilitating the analysis of deformation and failure in soils.

1. Soil is treated as a continuous material.
2. Soil particles are assumed to be sufficiently small.
3. The continuum assumption is particularly valid for cohesive and saturated soils.

1.5.5 Sign conventions for stresses

In soil mechanics, normal stresses are considered positive when they act in compression and negative when they act in tension.

- Compressive normal stress: $\sigma > 0$ mean σ_x , σ_y and σ_z are normal stresses; compression = '+' and Tensile normal stress: $\sigma < 0$, tension = "-"
- For shear stresses: is considered positive if it tends to rotate the soil element in a counter clockwise direction. τ_{xy} , τ_{yz} , τ_{zx} : (Counter clockwise rotation is "+").

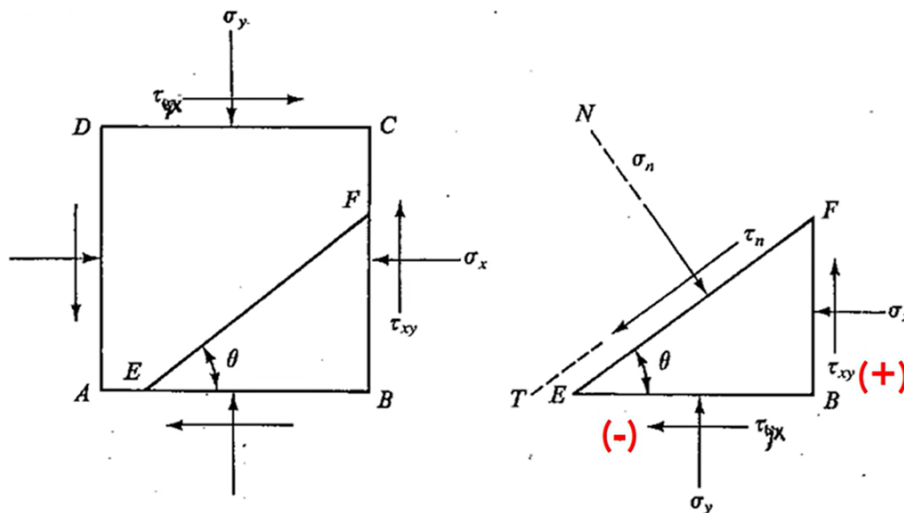


Figure 1.17: Direction of Stresses

1.5.6 transformation of plane stress

- Consider the conditions for equilibrium of a prismatic element with faces perpendicular to the x , y , and x' axes.

$$\sum F_x = 0 = \sigma_x \Delta A - \sigma_{x'} (\Delta A \cos \theta) \cos \theta - \tau_{x'y'} (\Delta A \cos \theta) \sin \theta - \sigma_y (\Delta A \sin \theta) \sin \theta - \tau_{xy} (\Delta A \sin \theta) \cos \theta \quad (1.4)$$

$$\sum F_y = 0 = \tau_{xy} \Delta A + \sigma_x (\Delta A \cos \theta) \sin \theta - \tau_{x'y'} (\Delta A \cos \theta) \cos \theta - \sigma_y (\Delta A \sin \theta) \cos \theta + \tau_{xy} (\Delta A \sin \theta) \sin \theta \quad (1.5)$$

- The above equations may be rewritten to yield the stress transformation relations:

$$\sigma_{x'} = \frac{\sigma_x + \sigma_y}{2} + \frac{\sigma_x - \sigma_y}{2} \cos 2\theta + \tau_{xy} \sin 2\theta \quad (1.6)$$

$$\sigma_{y'} = \frac{\sigma_x + \sigma_y}{2} - \frac{\sigma_x - \sigma_y}{2} \cos 2\theta - \tau_{xy} \sin 2\theta \quad (1.7)$$

$$\tau_{x'y'} = -\frac{\sigma_x - \sigma_y}{2} \sin 2\theta + \tau_{xy} \cos 2\theta \quad (1.8)$$

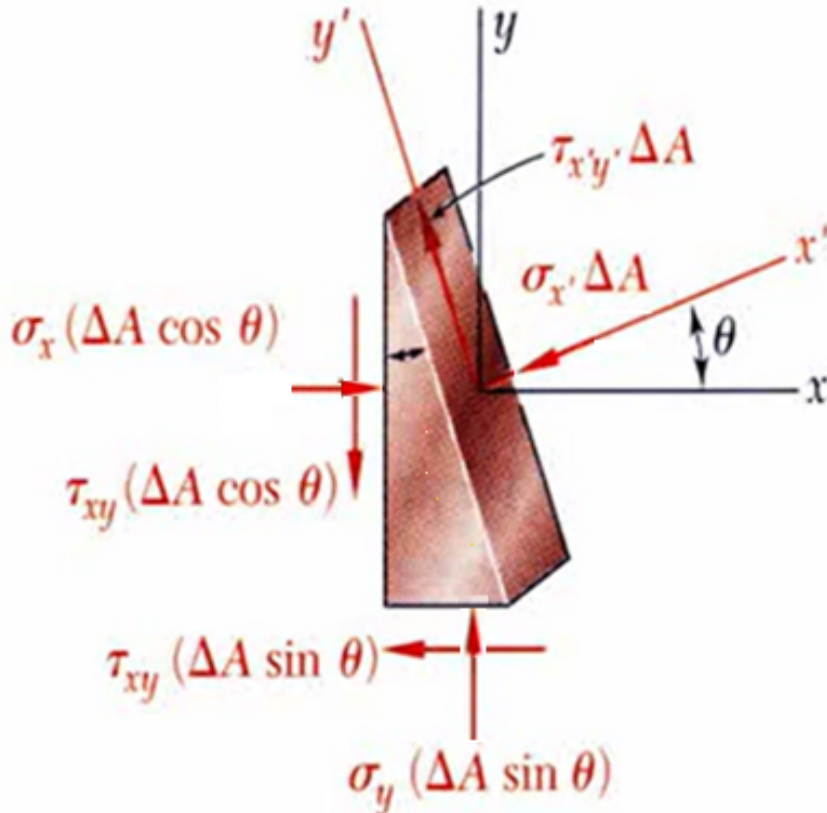


Figure 1.18: the stress transformation relations

Direct Calculation of Stresses in a soil:

$$\sigma_n = \frac{\sigma_y + \sigma_x}{2} + \frac{\sigma_y - \sigma_x}{2} \cos 2\theta + \tau_{xy} \sin 2\theta,$$

$$\tau_n = \frac{\sigma_y - \sigma_x}{2} \sin 2\theta - \tau_{xy} \cos 2\theta.$$

1.5.7 Direct Calculation of Principal Stresses and Plane Orientation

The principal stresses can be obtained directly from the stress components σ_x , σ_y , and τ_{xy} as follows:

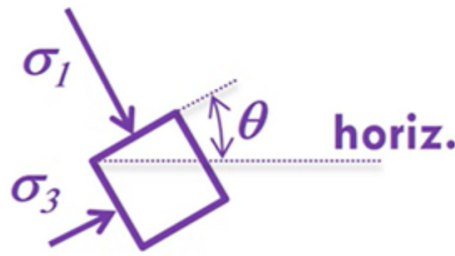


Figure 1.19

$$\sigma_1 = \frac{\sigma_x + \sigma_y}{2} + \sqrt{\left(\frac{\sigma_y - \sigma_x}{2}\right)^2 + \tau_{xy}^2} \quad (1.9)$$

$$\sigma_3 = \frac{\sigma_x + \sigma_y}{2} - \sqrt{\left(\frac{\sigma_y - \sigma_x}{2}\right)^2 + \tau_{xy}^2} \quad (1.10)$$

The orientation of the principal planes is given by

$$\tan 2\theta = \frac{2\tau_{xy}}{\sigma_y - \sigma_x} \quad (1.11)$$

To use these equations, the stress components σ_x , σ_y , and τ_{xy} must be known.

Problem

Consider the stresses acting on the element shown. Determine the normal stress σ_n and the shear stress τ acting on a plane inclined at an angle $\alpha = 35^\circ$ with respect to the horizontal.

Given:

$$\sigma_A = 52 \text{ kPa}, \quad \sigma_B = 12 \text{ kPa}$$

Solution

Assuming a plane stress state with:

$$\sigma_x = \sigma_A, \quad \sigma_y = \sigma_B, \quad \tau_{xy} = 0$$

The stress transformation equations are:

$$\sigma_n = \frac{\sigma_x + \sigma_y}{2} + \frac{\sigma_x - \sigma_y}{2} \cos(2\alpha)$$

$$\tau = -\frac{\sigma_x - \sigma_y}{2} \sin(2\alpha)$$

Substituting the given values:

$$\frac{\sigma_x + \sigma_y}{2} = \frac{52 + 12}{2} = 32 \text{ kPa}$$

$$\frac{\sigma_x - \sigma_y}{2} = \frac{52 - 12}{2} = 20 \text{ kPa}$$

$$\cos(2 \times 35^\circ) = \cos 70^\circ \approx 0.342$$

$$\sin(2 \times 35^\circ) = \sin 70^\circ \approx 0.94$$

Therefore:

$$\sigma_n = 32 + 20(0.342) = 38.84 \text{ kPa}$$

$$\tau = -20(0.94) = -18.8 \text{ kPa}$$

Results

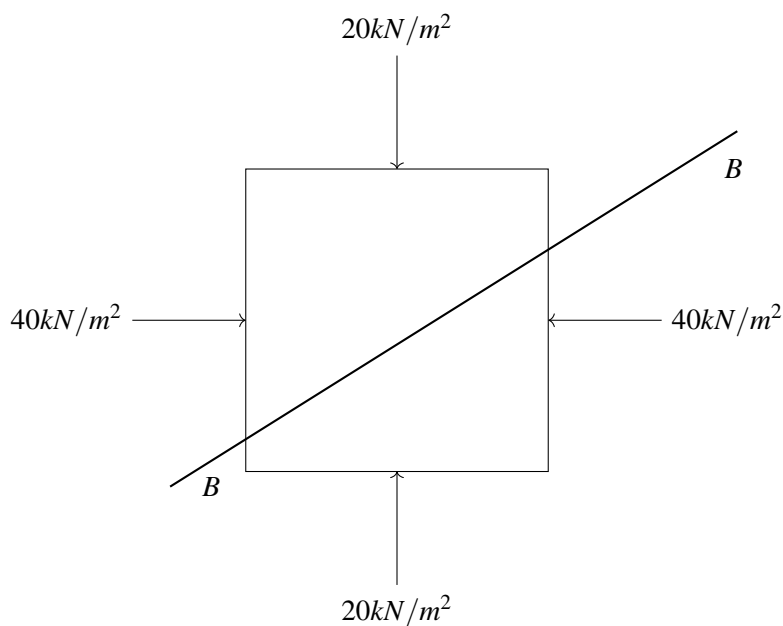
$$\sigma_n \approx 38.8 \text{ kPa}$$

$$|\tau| \approx 18.8 \text{ kPa}$$

Problem

For a given in figure find the stresses at plane B-B Case one: Given σ_1 and σ_3 , required σ_θ and τ_θ

Stress Element on Plane B-B



Stress on Plane B–B Using Mohr's Circle

Given

Principal stresses:

$$\sigma_1 = 40 \text{ kN/m}^2, \quad \sigma_3 = 20 \text{ kN/m}^2$$

Plane $B-B$ is inclined at 30° to the principal plane.

$$\Rightarrow \theta = 60^\circ$$

(since Mohr's circle uses the normal to the plane)

Objective

Find: σ_θ and τ_θ on plane $B-B$.

Method 1: Mohr's Circle (Graphical)

Step 1: Plot Principal Stress Points

$$A(\sigma_1, 0) = (40, 0), \quad C(\sigma_3, 0) = (20, 0)$$

Step 2: Determine Center and Radius

Center:

$$O = \left(\frac{\sigma_1 + \sigma_3}{2}, 0 \right) = (30, 0)$$

Radius:

$$R = \frac{\sigma_1 - \sigma_3}{2} = 10$$

Step 3: Draw Mohr's Circle

- Center at $(30, 0)$
- Radius = 10

Step 4: Locate Plane $B-B$

On Mohr's circle, rotate by:

$$2\theta = 2(60^\circ) = 120^\circ$$

from point A .

Step 5: Read Coordinates at Intersection

$$\sigma_\theta = 25 \text{ kN/m}^2$$

$$\tau_\theta = -8.7 \text{ kN/m}^2$$

Method 2: Analytical (Stress Transformation Equations)

Normal Stress

$$\sigma_{\theta} = \frac{\sigma_1 + \sigma_3}{2} + \frac{\sigma_1 - \sigma_3}{2} \cos(2\theta)$$

$$\sigma_{\theta} = \frac{40 + 20}{2} + \frac{40 - 20}{2} \cos(120^\circ)$$

$$\sigma_{\theta} = 30 - 5 = 25 \text{ kN/m}^2$$

Shear Stress

$$\tau_{\theta} = \frac{\sigma_1 - \sigma_3}{2} \sin(2\theta)$$

$$\tau_{\theta} = \frac{40 - 20}{2} \sin(120^\circ)$$

$$\tau_{\theta} = -8.66 \text{ kN/m}^2$$

(Negative sign indicates direction of shear)

Final Answer

$$\sigma_{\theta} = 25 \text{ kN/m}^2, \quad \tau_{\theta} = -8.7 \text{ kN/m}^2$$

Alternate Solution

1. Steps 1 and 2 are the same as above.
2. Draw line $C'C'$ through point $(40, 0)$ parallel to the plane on which stress $(40, 0)$ acts.
3. Line $C'C'$ intersects Mohr's circle only at $(40, 0)$, hence this is O_p .
4. Steps 5 and 6 are the same as above.

Analytical Solution

$$\sigma_{\theta} = \frac{\sigma_1 + \sigma_3}{2} + \frac{\sigma_1 - \sigma_3}{2} \cos(2\theta)$$

$$\sigma_{\theta} = \frac{40 + 20}{2} + \frac{40 - 20}{2} \cos(240^\circ) = 30 - 5 = 25 \text{ kN/m}^2$$

$$\tau_{\theta} = \frac{\sigma_1 - \sigma_3}{2} \sin(2\theta) = \frac{40 - 20}{2} \sin(240^\circ) = -8.66 \text{ kN/m}^2$$

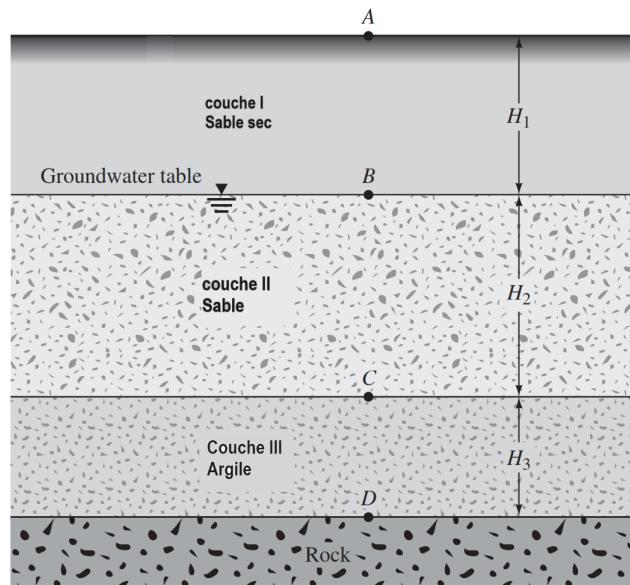
Final Answer

$$\sigma_{\theta} = 25 \text{ kN/m}^2, \quad \tau_{\theta} = -8.66 \text{ kN/m}^2$$

Example

A soil profile is shown in Figure 1. Calculate the values of the total stress σ , the pore water pressure u , and the effective stress σ' at points A, B, C, and D. The values are to be reported in the table provided.

N° couche	Épaisseurs (m)	Poids volumiques(kN/m ³)
I	$H_1 = 2$	$\gamma = 15$
II	$H_2 = 3$	$\gamma_{\text{sat}} = 17.8$
III	$H_3 = 7$	$\gamma_{\text{sat}} = 18.6$



Example

In order to determine the mechanical properties, a direct shear test is carried out on three soil samples. The results obtained at failure are summarized in the following table:

No de l'échantillon	1	2	3
Force Normale (N)	167.54	382.05	574.43
Force latérale (N)	511.89	617.12	701.46

Figure 1.20: Direct shear test

Determine the mechanical properties of the soil:

- Graphically, both by direct plotting and by linear regression; analytically; and compare the results.
- Determine the principal stresses at failure for each test, as well as the theoretical inclination angle of the shear plane with respect to the principal stress planes associated with σ_1 .

Solution – Example

Given data

A direct shear test was performed on three soil samples. The forces measured at failure are summarized below:

Sample No.	Normal force N (N)	Shear force T (N)
1	167.54	511.89
2	382.05	617.12
3	574.43	701.46

Let A be the area of the shear plane (assumed constant for all tests).

The normal and shear stresses at failure are:

$$\sigma = \frac{N}{A}, \quad \tau = \frac{T}{A}.$$

The Mohr–Coulomb failure criterion is:

$$\tau = c + \sigma \tan \varphi.$$

Multiplying by A , the equation becomes:

$$T = cA + N \tan \varphi.$$

Substituting the experimental values:

$$\tan \varphi \approx \frac{617.12 - 511.89}{382.05 - 167.54} = 0.4.$$

Hence, the friction angle is:

$$\varphi = \arctan(0.4) \approx 21.4^\circ$$

2) Analytical determination

Using two tests (i, j), the friction angle can be estimated analytically as:

$$\tan \varphi = \frac{T_2 - T_1}{N_2 - N_1}.$$

For samples 1 and 3:

$$\tan \varphi = \frac{701.46 - 511.89}{574.43 - 167.54} \approx 0.466,$$

$$\varphi \approx 25^\circ.$$

The small difference compared with the regression result is due to experimental scatter. The regression value is considered more representative.

3) Inclination angle of the failure plane

According to Mohr–Coulomb theory, the theoretical inclination of the failure plane with respect to the major principal stress direction σ_1 is:

$$\theta = 45^\circ + \frac{\varphi}{2}$$

Using $\varphi = 21.4^\circ$:

$$\theta \approx 45^\circ + 10.7^\circ = 55.7^\circ.$$

Summary

$$\varphi \approx 21.4^\circ,$$

$$\theta \approx 55.7^\circ.$$

Remark The friction angle obtained by linear regression is the most reliable value. The exact value of the cohesion depends on the shear box area A .

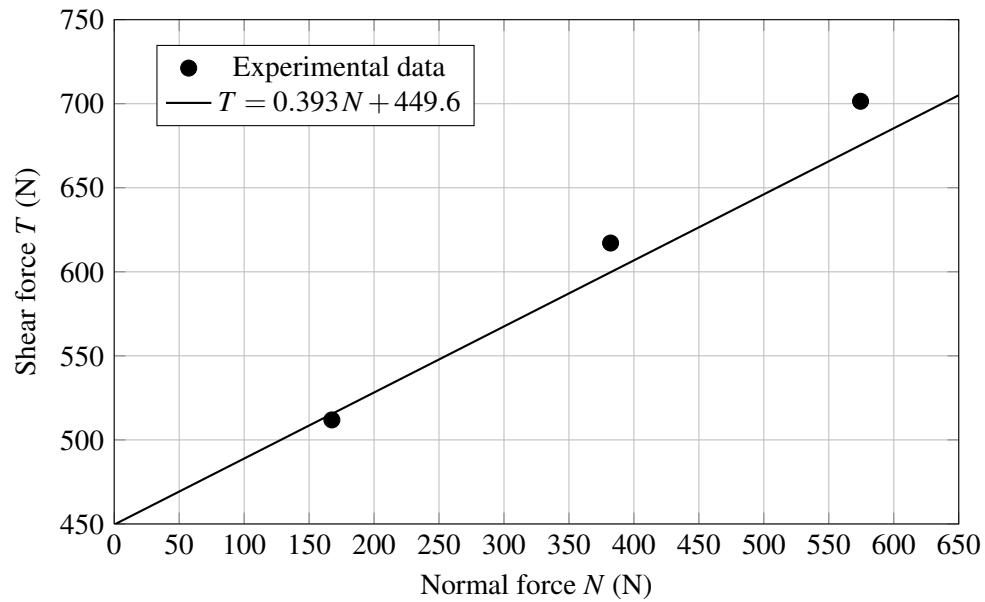


Figure 1.21: Direct shear test: shear force versus normal force

Exercise 3: Unconfined compressive strength from a CU triaxial test

Given data

- CU triaxial test on a low-plasticity clay
- Dry unit weight: $\gamma_d = 17 \text{ kN/m}^3$
- Depth of sampling: $z = 8.15 \text{ m}$
- Porosity: $n = 0.35$
- Triaxial test results: $\phi_{cu} = 14^\circ$, $C_{cu} = 40 \text{ kPa}$

Step 1: Determine the vertical effective stress at sampling depth

The total vertical stress at depth z is:

$$\sigma_v = \gamma z$$

The saturated unit weight γ_{sat} is:

$$\gamma_{\text{sat}} = \gamma_d(1 + w)$$

where w is the water content. Alternatively, using porosity n and assuming full saturation:

$$\gamma_{\text{sat}} = \gamma_d(1 + n) \approx 17 \times (1 + 0.35) \approx 22.95 \text{ kN/m}^3$$

The vertical stress at depth:

$$\sigma_v = \gamma_{\text{sat}} \cdot z \approx 22.95 \times 8.15 \approx 187 \text{ kPa}$$

Step 2: Relate CU triaxial results to unconfined compressive strength

For a CU (Consolidated Undrained) triaxial test on a saturated clay, the **uniaxial compressive strength** $q_u = R_c$ is related to the cohesion and internal friction angle:

$$q_u = 2C_{cu} \cos \phi_{cu} / (1 - \sin \phi_{cu})$$

Substitute values (convert degrees to radians if needed):

$$\phi_{cu} = 14^\circ, \quad C_{cu} = 40 \text{ kPa}$$

$$\begin{aligned} q_u &= \frac{2 \times 40 \times \cos 14^\circ}{1 - \sin 14^\circ} \\ &= \frac{80 \times 0.970}{1 - 0.242} \\ &= \frac{77.6}{0.758} \\ &\approx 102.4 \text{ kPa} \end{aligned}$$

Step 3: Conclusion

The estimated unconfined compressive strength of the saturated clay sample is:

$$q_u \approx 102 \text{ kPa}$$

Remark: This assumes that the sample remained fully saturated and that the CU triaxial test results are representative of in-situ conditions.

Exercise

Assuming that the stress and strain fields are homogeneous, study how the Mohr circle and the directions of the principal stresses evolve during a direct shear test using the Casagrande shear box and during a triaxial test. What conclusions can be drawn?

Exercise: Mohr Circle and Principal Stress Directions

1. General Assumptions

- Stress and strain fields are assumed homogeneous.
- Soil behavior is analyzed using effective stresses.
- Failure is interpreted using the Mohr–Coulomb criterion.

2. Direct Shear Test (Casagrande Shear Box)

Stress state: Constant normal stress σ_n on a predefined shear plane; shear stress τ increases until failure.

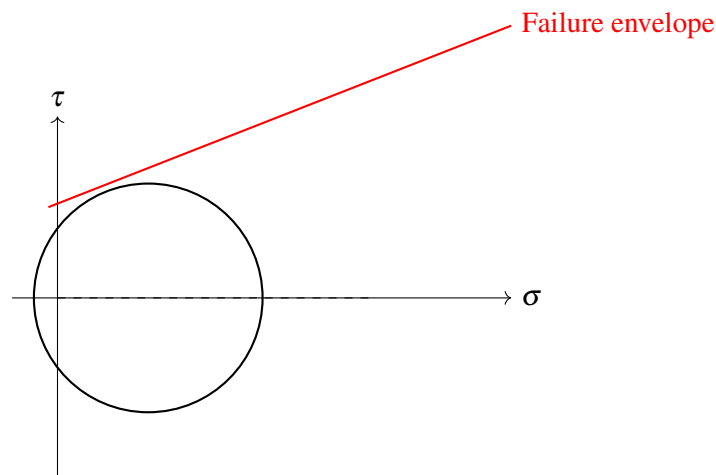
Mohr circle evolution:

- One point of the Mohr circle is fixed at σ_n .
- The radius increases as τ increases.
- Failure occurs when the circle touches the Mohr-Coulomb envelope.

Principal stresses and directions:

- Principal stresses rotate during loading.
- The failure plane is imposed by the apparatus.

Mohr Circle Sketch:



3. Triaxial Test

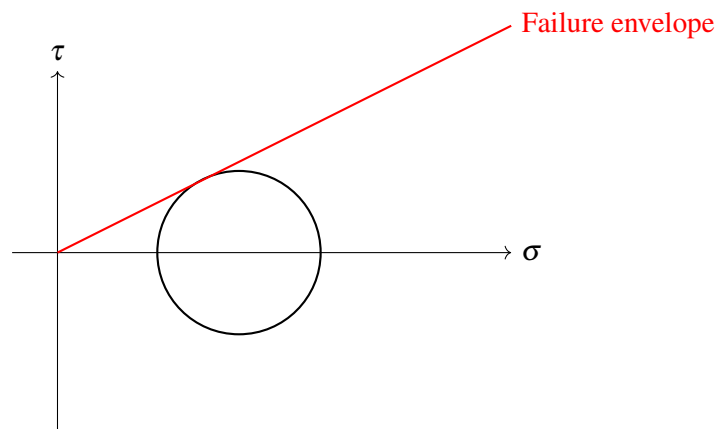
Stress state: Axisymmetric with σ_1 major principal stress and $\sigma_2 = \sigma_3$ minor stresses.

Mohr circle evolution:

- Circle grows as σ_1 increases.
- Principal stress directions remain fixed.
- Failure occurs when the circle touches the failure envelope.

Failure plane inclination:

$$\theta = 45^\circ + \frac{\phi}{2}$$

Mohr Circle Sketch:**4. Comparison and Conclusions**

Aspect	Direct Shear	Triaxial Test
Stress state	Non-uniform	Uniform
Failure plane	Imposed	Natural
Principal stress directions	Rotate	Fixed
Mohr circle evolution	Expansion with rotation	Expansion without rotation
Reliability of parameters	Moderate	High

Conclusion: The triaxial test provides a realistic stress state and natural failure plane, yielding more reliable shear strength parameters. The direct shear test is simpler but imposes artificial boundary conditions, affecting stress paths and failure.

Example

The consolidated drained triaxial tests on two soil samples gave the following results:

Test No.	Confining stress σ_3 , kN/m ²	Deviator stress at failure $\sigma_d = \sigma_1 - \sigma_3$, kN/m ²
1	70	173
2	105	235

Table 1.2: Results of CD triaxial tests

Determine the soil shear strength parameters, knowing that:

$$\sigma'_1 = \sigma'_3 \tan^2 \left(\frac{\pi}{4} + \frac{\phi'}{2} \right) + 2c' \tan \left(\frac{\pi}{4} + \frac{\phi'}{2} \right)$$

1.5.8 Plane Representation – Mohr's Circle

For the study of the state of stress around a point Representation of stresses in a coordinate system (τ, σ) :

- The horizontal axis coincides with the normal stress σ acting on the plane.
- The vertical axis coincides with the tangential (shear) stress τ
- A positive rotation of the plane by an angle $\pi/2$ is measured with respect to the σ axis. When the plane rotates about point M, the representative point of the stresses traces a circle known as the Mohr circle.

In three-dimensional stress analysis, three Mohr circles appear, defined by:

σ_1 : major principal stress,

σ_2 : intermediate principal stress,

σ_3 : minor principal stress.

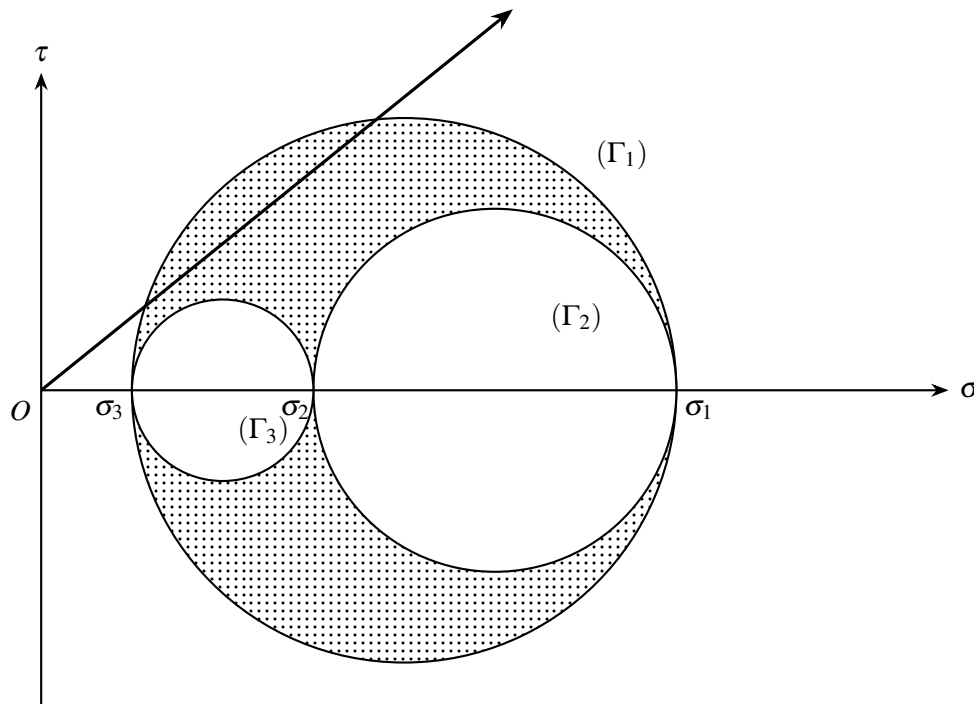
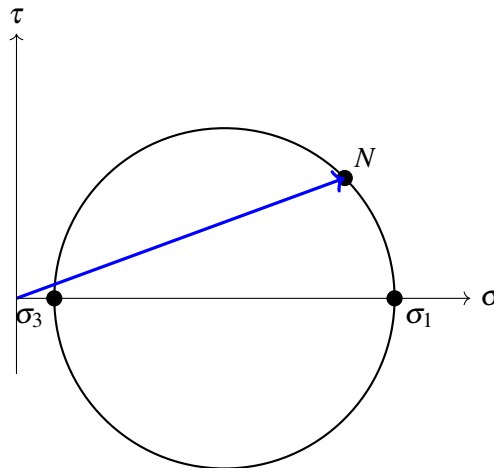


Figure 1.22: three Mohr circles, $\sigma_1, \sigma_2, \sigma_3$

1.5.9 Two-Dimensional Problems

In most cases, measured in meters (Mds), the majority of problems are two-dimensional (2D). Axisymmetric Problems: circular foundations, piles. Geometry constant in one direction: slopes, embankments, strip footings, walls. The studied plane contains σ_1 and σ_3 .

Reduction of Mohr's graphical representation to a single plane circle perpendicular to σ For a given stress state, when the facet rotates around point M, the stresses are represented by a point N on Mohr's circle.



Important property of Mohr's circles: When a facet rotates about point M, the point N representing the stresses on Mohr's circle rotates in the opposite direction with twice the angular speed.

1.5.10 Shear Strength of Soils

1.5.10.1 Shear Strength of Soil and Mohr-Coulomb Theory

The shear strength of soil represents its resistance to shear failure and is commonly expressed using the Mohr–Coulomb failure criterion:

$$\tau = c + \sigma \tan \varphi \quad (1.12)$$

where:

- τ is the shear strength,
- c is the cohesion,
- σ is the normal stress,
- φ is the angle of internal friction.

Clay soils generally exhibit high cohesion and low friction angle, while sandy soils have negligible cohesion and a high friction angle.

1.5.11 Relationship Between Plasticity and Shear Strength

An increase in water content reduces effective stress and consequently decreases shear strength. Highly plastic clays are therefore more sensitive to moisture variations and may experience stability problems such as slope failure or bearing capacity reduction.

1.6 Linear Elasticity – Stress–Strain Relationships (Elastic Domain)

Field of Application: Roads, highways, airport runways, rock masses, dam foundations and abutments, bridge piers, tunnel convergence, etc. Fundamental Constitutive Laws (Material Laws): Stress–Strain Relationships ($\sigma - \varepsilon$)

1.6.1 Basic Concepts of Elasticity (Review)

Linear elastic behavior is characterized by the reversibility of deformations. According to Hooke's law, the mechanical response of the material is completely described by two independent elastic constants: the Young's modulus (E) and the Poisson's ratio (ν).



Figure 1.23: Field of Application: Linear Elasticity

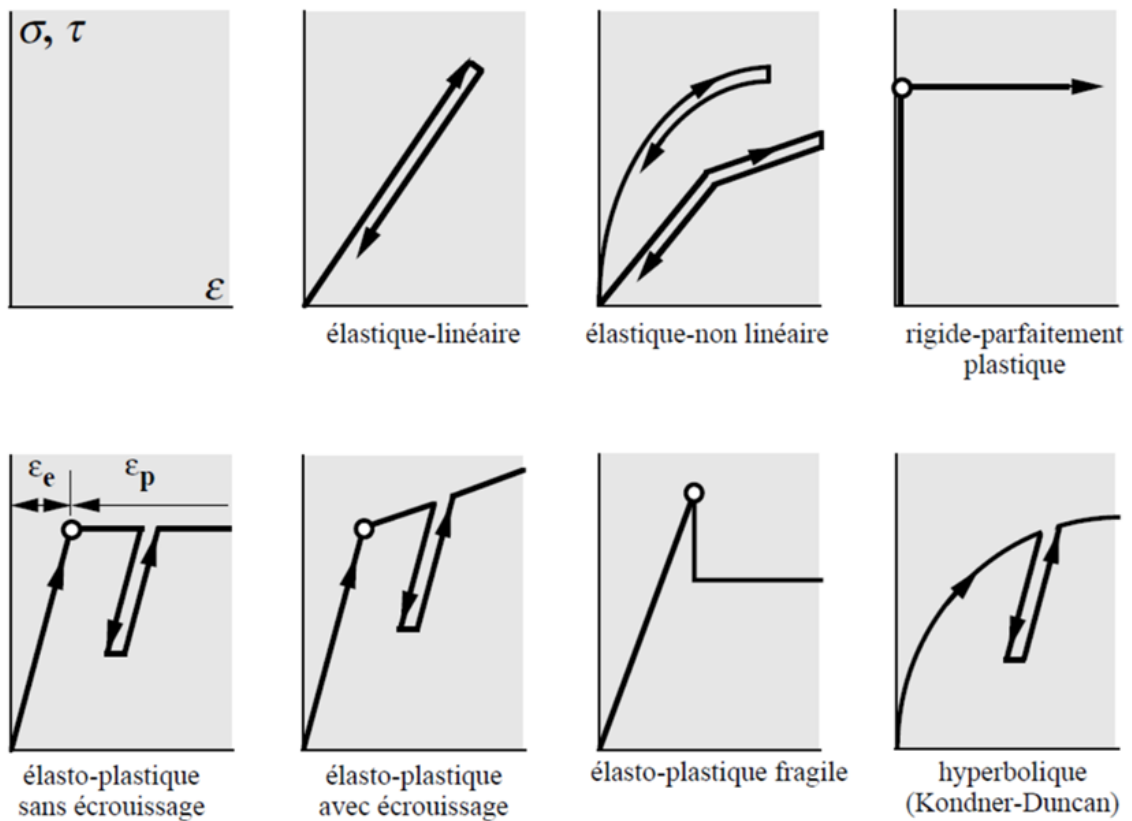


Figure 1.24: Failure Criterion (Yield Criterion / Plasticity Law): Mohr–Coulomb, Drucker–Prager, von Mises

1.6.2 Equivalent Linear Elastic Behavior

Equivalent Linear Elastic Behavior is a simplified representation of soil or material behavior where nonlinear or time-dependent effects are approximated by an “equivalent” linear elastic response using effective parameters (e.g., modulus and Poisson’s ratio).

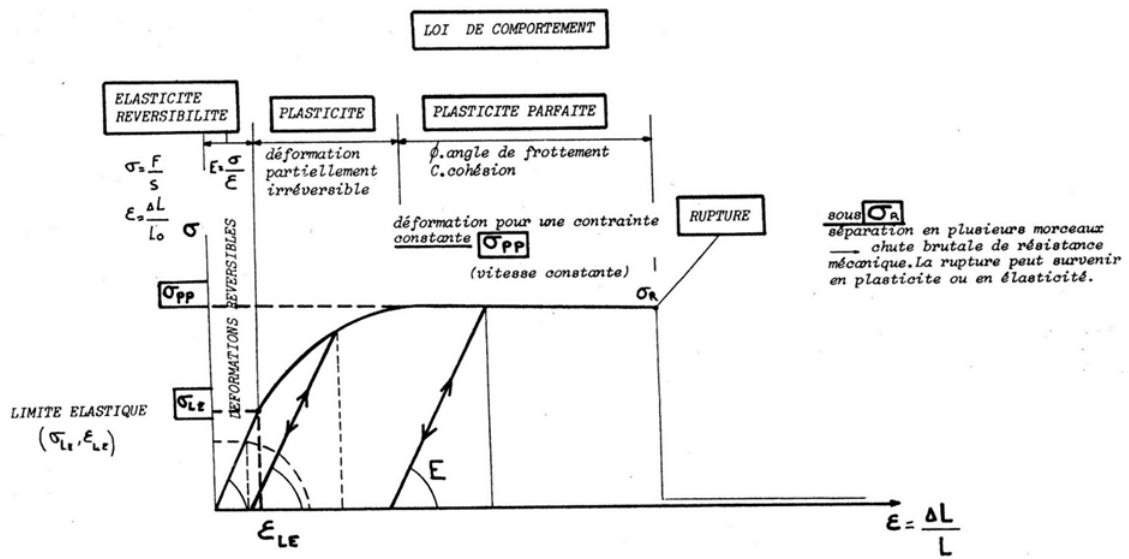


Figure 1.25: Overview of the Principal Aspects of Soil Behavior

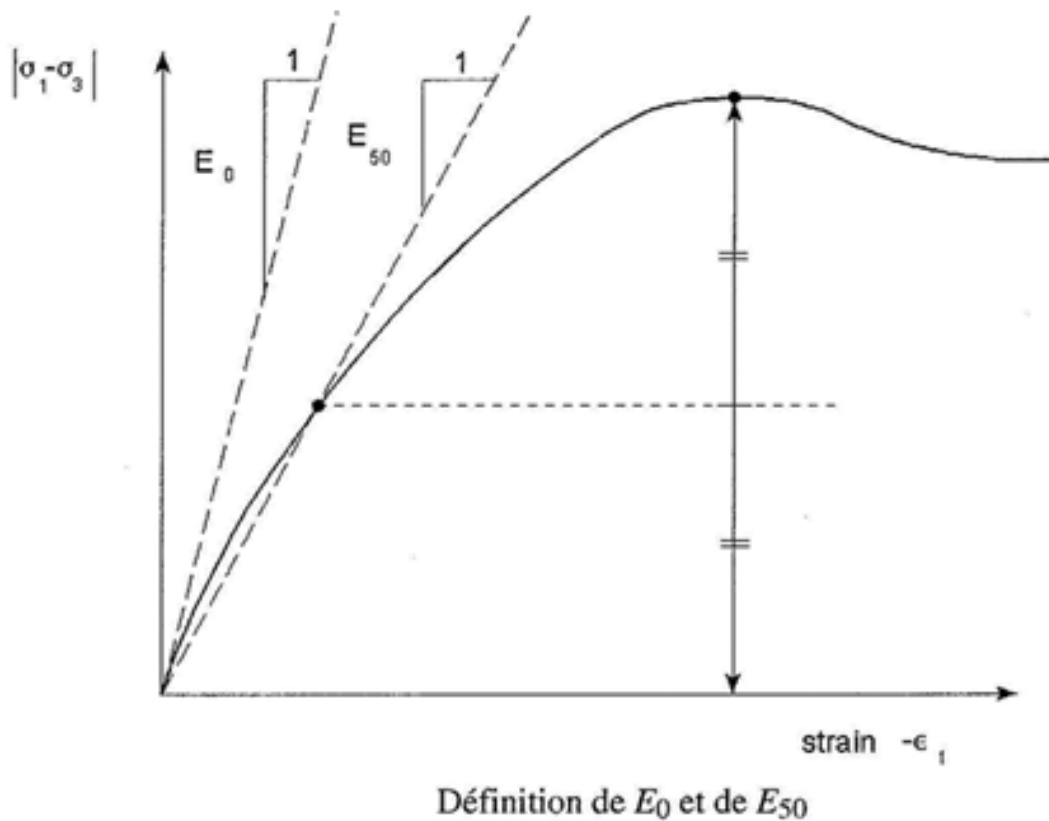


Figure 1.26: Equivalent Linear Elastic Behavior

The real behavior of soils is neither purely elastic nor linear. For soils, both the initial modulus and the secant modulus tend to increase with the confining pressure. As a result, deeper soil layers often exhibit higher stiffness than surface layers.

1.6.3 Practical Considerations for Linear Elastic Representation of Soils

When choosing a **constant deformation modulus** to represent soil behavior, the selected value should account for both the **stress level** and the **stress path**.

Nevertheless, **linear elasticity based on the secant modulus** is often used in calculations for typical structures, for both static and dynamic problems. This approach provides reasonable results as long as the stress level is properly estimated.

For example:

- Using E_{50} obtained from a *simple compression test* on clays can be acceptable if the **factor of safety** is approximately

$$F_s = \frac{q_{\max}}{q_{50}} \approx 2$$

- For **heavily overconsolidated clays** and some rocks with a **wide elastic range**, it is realistic to use E_0
- For **sands** and **normally consolidated clays**, it is preferable to use E_{50}

1.7 Stress Paths in (σ, ε) and (p, q) Spaces

Stress paths provide a compact way to describe how a material point evolves during loading, unloading, and reloading. They are commonly represented in: (i) the *stress–strain* plane (σ, ε) , and (ii) the *stress-invariant* plane (p, q) , where the same loading history can be interpreted in terms of mean stress and deviatoric stress.

1.7.1 Stress path in the (σ, ε) plane

In the (σ, ε) representation, the path shows the relationship between an applied stress measure (e.g., axial stress σ) and the corresponding strain ε . Typical features include a loading branch, possible yielding (change in slope), and unloading/reloading hysteresis in inelastic materials.

1.7.2 Stress path in the (p, q) plane

For many constitutive models (especially in soil and rock mechanics), stress paths are more naturally described using stress invariants:

$$p = \frac{\sigma_1 + \sigma_2 + \sigma_3}{3}, \quad (1.13)$$

$$q = \sqrt{\frac{3}{2} \mathbf{s} : \mathbf{s}}, \quad (1.14)$$

where \mathbf{s} is the deviatoric stress tensor. In conventional triaxial conditions ($\sigma_2 = \sigma_3$), a common equivalent is:

$$q = \sigma_1 - \sigma_3. \quad (1.15)$$

In the (p, q) plane:

- **Isotropic compression** increases p at (approximately) $q \approx 0$.
- **Triaxial shearing at constant confinement** often increases both p and q .
- **Pure shear at constant mean stress** is an (idealized) path with $p = \text{const}$ and increasing q .



2. Behavior of Fine-Grained Soils

Fine-grained soils (silts and clays) exhibit mechanical and hydraulic behaviors that are strongly controlled by their small particle size, surface forces, mineralogy, and pore-water chemistry. Unlike coarse-grained soils, their response is often time-dependent and highly sensitive to changes in water content, effective stress, and fabric (microstructure).

2.1 Nature and Classification

Fine-grained soils are commonly classified using particle size distribution and plasticity. The *Atterberg limits* (liquid limit w_L , plastic limit w_P , and plasticity index $I_P = w_L - w_P$) quantify the consistency changes with water content and provide a practical indicator of engineering behavior.

2.2 Microstructure and Physico-Chemical Effects

Clay particles are platy and carry surface charges, which attract water molecules and exchangeable cations. This leads to:

- **Diffuse double layer effects** that influence interparticle forces and compressibility,
- **Fabric anisotropy** (preferred particle orientation) affecting stiffness and strength,
- **Sensitivity to salinity and pore-water chemistry** (especially in active clays such as montmorillonite).

2.3 Effective Stress and Pore Pressure

The behavior of saturated fine-grained soils is governed by effective stress:

$$\sigma' = \sigma - u, \quad (2.1)$$

where σ is total stress and u is pore-water pressure. Because permeability is low, loading may generate significant excess pore pressure, making undrained behavior particularly important in short-term conditions.



Figure 2.1: fine-grained soils (clay microstructure).

2.4 Compressibility and Consolidation

2.4.1 One-Dimensional Compression

Under one-dimensional loading, volume change is often described with the void ratio e versus logarithm of effective vertical stress σ'_v . Two key parameters are:

- **Compression index** C_c (virgin compression slope),
- **Recompression index** C_r (unloading/reloading slope).

2.4.2 Primary Consolidation

Consolidation is the time-dependent settlement caused by dissipation of excess pore pressure. Terzaghi's one-dimensional consolidation theory introduces the coefficient of consolidation:

$$c_v = \frac{k}{m_v \gamma_w}, \quad (2.2)$$

where k is permeability, m_v is coefficient of volume compressibility, and γ_w is unit weight of water.

2.4.3 Secondary Compression (Creep)

After primary consolidation, many clays continue to deform at approximately constant effective stress due to creep. This is captured by the secondary compression index C_α and becomes critical for long-term settlement of structures on soft clays.

2.5 Shear Strength of Fine-Grained Soils

2.5.1 Drained Strength

In drained conditions (slow loading), pore pressure has time to dissipate and strength is expressed using effective stress:

$$\tau_f = c' + \sigma' \tan \phi', \quad (2.3)$$

where c' is effective cohesion (often small for normally consolidated clays) and ϕ' is the effective friction angle.

2.5.2 Undrained Strength

In undrained conditions (rapid loading), volume change is constrained and strength is commonly represented by:

$$\tau_f = s_u, \tag{2.4}$$

where s_u is undrained shear strength. The value of s_u depends on stress history (OCR), plasticity, and structure. Normally consolidated clays typically exhibit lower s_u than overconsolidated clays at the same current stress level.

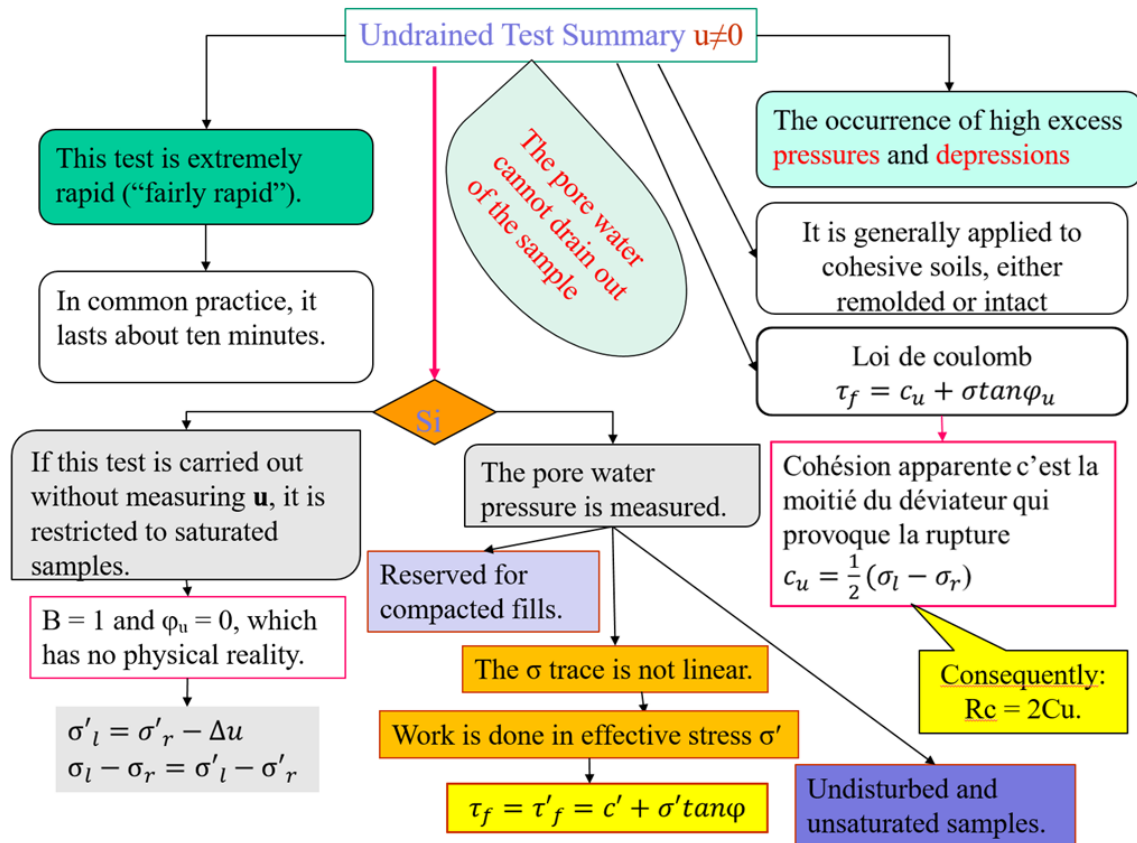


Figure 2.2: undrained shear strength

2.6 Stress History and Overconsolidation

A key concept for clays is the preconsolidation stress σ'_p (maximum past effective stress). The overconsolidation ratio (OCR) is:

$$OCR = \frac{\sigma'_p}{\sigma'_0}, \tag{2.5}$$

where σ'_0 is the current effective stress. Overconsolidated clays tend to be stiffer, dilative (in shear), and may develop negative pore pressures under undrained loading.

2.7 Permeability and Hydraulic Conductivity

Fine-grained soils have very low permeability due to small pore sizes. Hydraulic conductivity typically decreases with increasing plasticity and decreasing void ratio. This low permeability explains why consolidation and pore-pressure dissipation can take months or years in the field.

2.8 Shrink–Swell Behavior

Active clays can undergo significant volume change with moisture variation. Swelling pressure and shrinkage cracking may cause:

- heave of lightly loaded structures,
- damage to pavements and shallow foundations,
- increased permeability through fissures and desiccation cracks.

2.9 Sensitivity and Structure

Some natural clays possess bonding or cementation and are termed *structured clays*. When remolded, they may lose a large fraction of their strength; this is quantified by sensitivity:

$$S_t = \frac{s_u(\text{undisturbed})}{s_u(\text{remolded})}. \quad (2.6)$$

Highly sensitive clays (quick clays) can fail suddenly and flow-like once disturbed.

2.10 Laboratory and Field Testing

Common tests for fine-grained soils include:

- **Atterberg limits** (index properties),
- **Oedometer test** (compressibility and consolidation parameters),
- **Triaxial tests** (UU, CU, CD) for strength and pore pressure response,
- **Vane shear test** (undrained strength in soft clays),
- **CPTu** (cone penetration with pore pressure) for profiling and interpretation of s_u and OCR.

Exercice

L'analyse des résultats des essais triaxiaux consolidés drainés CD sont résumés dans le tableaux suivant:

Essai	1	2	3
la contrainte latérale σ_3 (kPa)	100	200	300
le déviateur à la rupture $(\sigma_1 - \sigma_3)_r$ (kPa)	220	448	654

- tracer le cercle de Mohr pour les 3 échantillons
- Dessiner l'enveloppe de la rupture
- déterminer les paramètres de la résistance du sol

Consolidated Drained (CD) Triaxial Test Results

The results of the CD triaxial tests are summarized in the following table:

Test	1	2	3
Lateral stress σ_3 (kPa)	100	200	300
Deviator stress at failure $(\sigma_1 - \sigma_3)_f$ (kPa)	220	448	654

Table 2.1: Summary of CD triaxial test results

Tasks

- Plot the Mohr circles for the three samples.
- Draw the failure envelope.

- Determine the soil strength parameters (cohesion c and friction angle ϕ).

Solution example

L'essai de consolidation drainé donnera les paramètres des contraintes effectives, puisque la pression interstitielle $u=0$ à la fin de l'essai, d'où $\sigma' = \sigma - u$

Essai	1	2	3
la contrainte latérale σ_3 (kPa)	100	200	300
le déviateur à la rupture $(\sigma_1 - \sigma_3)_r$ (kPa)	220	448	654
$(\sigma_1 = \sigma'_1)$ (kPa)	320	648	954

$$\sigma' = \sigma - 0$$

$$\sigma' = \sigma$$

$$\sigma' = \sigma_1$$

$$\sigma'_3 = \sigma_3$$

Remark A rigorous determination of the parameters c' and ϕ' requires several triaxial tests performed under different confining pressures in order to define the Mohr-Coulomb failure envelope in effective stresses

Solution:

$$\sigma_1 = \sigma_3 + (\Delta\sigma) = 84 + 63,7 = 147,7$$

$$\sigma_1 = \sigma_3 \tan^2\left(45^\circ + \frac{\phi}{2}\right) + 2c \cdot \tan\left(45^\circ + \frac{\phi}{2}\right) =$$

$$\sigma_3 \tan^2\left(45^\circ + \frac{\phi}{2}\right) + \frac{\phi}{2} cu = 2\sigma_3 \tan\left(45^\circ + \frac{\phi}{2}\right) + \phi cu = \tan^{-1}$$

$$\left(\frac{\sigma_1}{\sigma_3}\right)$$

$$0,5 = \tan^{-1}\left(\frac{147,7}{84}\right) - 0,5 = 52,9^\circ \quad \phi_{cu} = 16$$

$$\sigma'_1 - 1 = \sigma_1 - \Delta u_d = 147,7 - 47,6 = 100,1 \quad \sigma'_3 = \sigma_3 - \Delta u_d = 84 - 47,6 = 36,4$$

$$\sigma_1 = \sigma_3 \tan^2\left(45^\circ + \frac{\phi}{2}\right) + 2c \tan\left(45^\circ + \frac{\phi}{2}\right) = \sigma_3 \tan^2\left(45^\circ + \frac{\phi}{2}\right)$$

$$45^\circ + \frac{\phi}{2} = \tan^{-1}\left[\left(\frac{\sigma_1}{\sigma_3}\right)^{0,5}\right] = \tan^{-1}\left[\left(\frac{100,1}{36,4}\right)^{0,5}\right] = 58,90^\circ \quad \phi_{cu} = 27,8^\circ$$

Example

A consolidated undrained shear test is carried out on a normally consolidated clay sample, yielding the following results: confining pressure $\sigma_3 = 84 \text{ kPa}$, final deviator stress $(\Delta\sigma_d)_f = 63,7 \text{ kPa}$; and final pore water pressure $(\Delta u_d)_f = 47,6 \text{ kPa}$

- Determine the total friction angle ϕ_{cu} and the effective (drained) friction angle ϕ' ;
- Determine the shear strength.

Solution

1) Final principal stresses

The final total axial stress is given by:

$$\sigma_1 = \sigma_3 + (\Delta\sigma_d)_f = 84 + 63,7 = 147,7 \text{ kPa.}$$

The final pore water pressure (pressure increment) is:

$$u_f = (\Delta u_d)_f = 47,6 \text{ kPa.}$$

The final effective stresses are therefore:

$$\sigma'_3 = \sigma_3 - u_f = 84 - 47.6 = 36.4 \text{ kPa,}$$

$$\sigma'_1 = \sigma_1 - u_f = 147.7 - 47.6 = 100.1 \text{ kPa.}$$

It can be verified that:

$$\sigma'_1 - \sigma'_3 = 100.1 - 36.4 = 63.7 \text{ kPa} = (\Delta\sigma_d)_f.$$

2) Total friction angle φ_{cu}

Using total stresses and assuming a Mohr–Coulomb failure criterion with zero cohesion, the following relation applies:

$$\sin \varphi_{cu} = \frac{\sigma_1 - \sigma_3}{\sigma_1 + \sigma_3}.$$

$$\sin \varphi_{cu} = \frac{147.7 - 84}{147.7 + 84} = \frac{63.7}{231.7} = 0.275.$$

Hence:

$$\varphi_{cu} = \arcsin(0.275) \approx 15.96^\circ \approx \boxed{16.0^\circ}.$$

3) Drained (effective) friction angle φ'

Using effective stresses:

$$\sin \varphi' = \frac{\sigma'_1 - \sigma'_3}{\sigma'_1 + \sigma'_3} = \frac{63.7}{100.1 + 36.4} = \frac{63.7}{136.5} = 0.47.$$

Therefore:

$$\varphi' = \arcsin(0.47) \approx 27.82^\circ \approx \boxed{27.8^\circ}.$$

4) Shear strength

- **Undrained shear strength** (CU test, total stress):

$$s_u = \frac{\sigma_1 - \sigma_3}{2} = \frac{63.7}{2} = 31.85 \text{ kPa} \approx \boxed{31.9 \text{ kPa}}.$$

- **Maximum effective shear strength:**

$$\tau_{\max} = \frac{\sigma'_1 - \sigma'_3}{2} = 31.85 \text{ kPa.}$$

The mean normal stress on the failure plane is:

$$\sigma_n = \frac{\sigma'_1 + \sigma'_3}{2} = 68.25 \text{ kPa.}$$

Using the Mohr–Coulomb criterion:

$$\tau = c' + \sigma_n \tan \varphi',$$

the implied effective cohesion is:

$$c' = \tau_{\max} - \sigma_n \tan \varphi' \approx 31.85 - 68.25 \tan(27.82^\circ) \approx -4.16 \text{ kPa.}$$

Summary

$$\varphi_{cu} \approx 16.0^\circ,$$

$$\varphi' \approx 27.8^\circ,$$

$$s_u \approx 31.9 \text{ kPa.}$$



3. Behavior of Granular Materials

3.1 Dilatancy and Contractancy of Granular Media

Granular soils exhibit volume changes under shear, which are critical in soil mechanics:

- **Dilatancy:** The tendency of a dense granular soil to **increase in volume** when sheared.
- **Contractancy:** The tendency of a loose granular soil to **decrease in volume** when sheared.

These behaviors significantly affect **shear strength, settlement, and stability** of soils.

In soil mechanics, the characteristic state refers to a specific stress–strain condition during shearing at which a soil exhibits constant volume behavior (neither dilatancy nor contraction occurs) and the shear stress reaches a steady value.

- For dense soils, it is the state at which the tendency to dilate is exactly balanced by the applied stress.
- For loose soils, it is the state at which contraction ceases and steady shear occurs.

3.2 Dilatancy Theory

Dilatancy refers to the tendency of dense granular soils to **expand in volume** when subjected to shear. Loose soils, on the other hand, tend to **contract** under shear. This behavior influences the **shear strength, settlement, and stability** of soils. The degree of dilatancy depends on **initial density, confining pressure, and stress path**. Understanding dilatancy is crucial for **earth structures, retaining walls, and foundation design**.

3.3 Critical State and Characteristic State

The **critical state** is reached when a soil deforms continuously at a **constant volume** and **constant shear stress**. The **characteristic state** is a specific condition where the soil exhibits neither dilation nor contraction under shear. These concepts form the basis of **critical state soil mechanics** and are fundamental in constitutive models such as the *Cam-clay model*. At the critical state, the soil's **shear stress and void ratio** remain constant despite ongoing deformation.

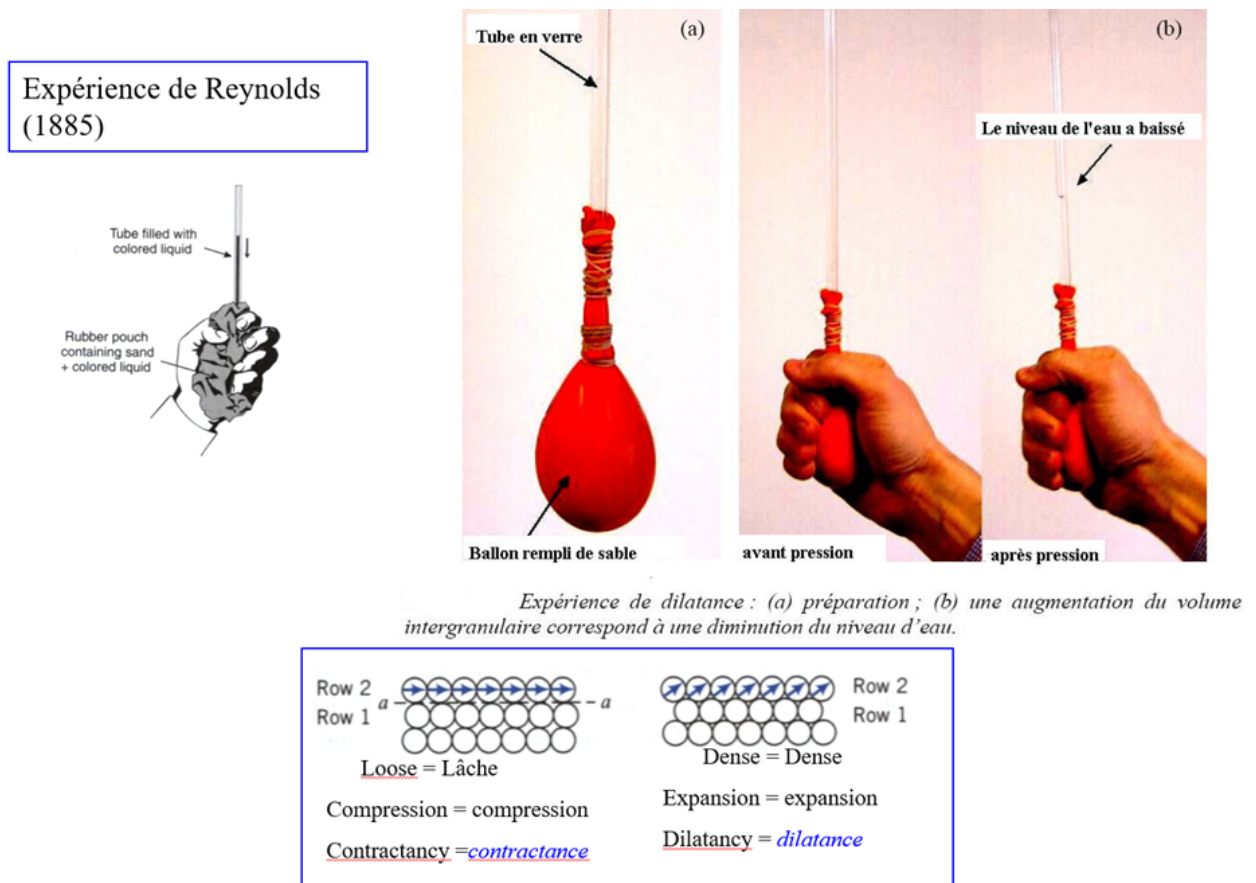


Figure 3.1: Dilatancy and Contractancy of Granular Media

3.4 Influence of Lateral Stress

The ratio of **lateral to vertical stress** ($K = \sigma_h / \sigma_v$) significantly affects soil behavior.

- **High lateral stress:** increases stiffness and shear strength, reducing the tendency for dilatancy.
- **Low lateral stress:** may promote dilation or contraction, especially in loose soils.

Lateral stress effects are particularly important in **tunnel convergence, retaining structures, and deep foundations**.

3.5 Behavior under Cyclic Loading: Contraction, Dilation, and Liquefaction

Soils subjected to **repeated loading**, such as during earthquakes or traffic, exhibit volume changes that influence stability:

- **Contraction:** Loose soils compress under cyclic loading, increasing **pore water pressure**.
- **Dilation:** Dense soils expand under cyclic shear, temporarily reducing pore water pressure.
- **Liquefaction:** Under certain conditions, particularly in loose saturated sands, cyclic loading may cause a **loss of shear strength** and flow-like behavior.

Understanding these behaviors is essential for the **design of earthquake-resistant foundations, embankments, and retaining structures**.

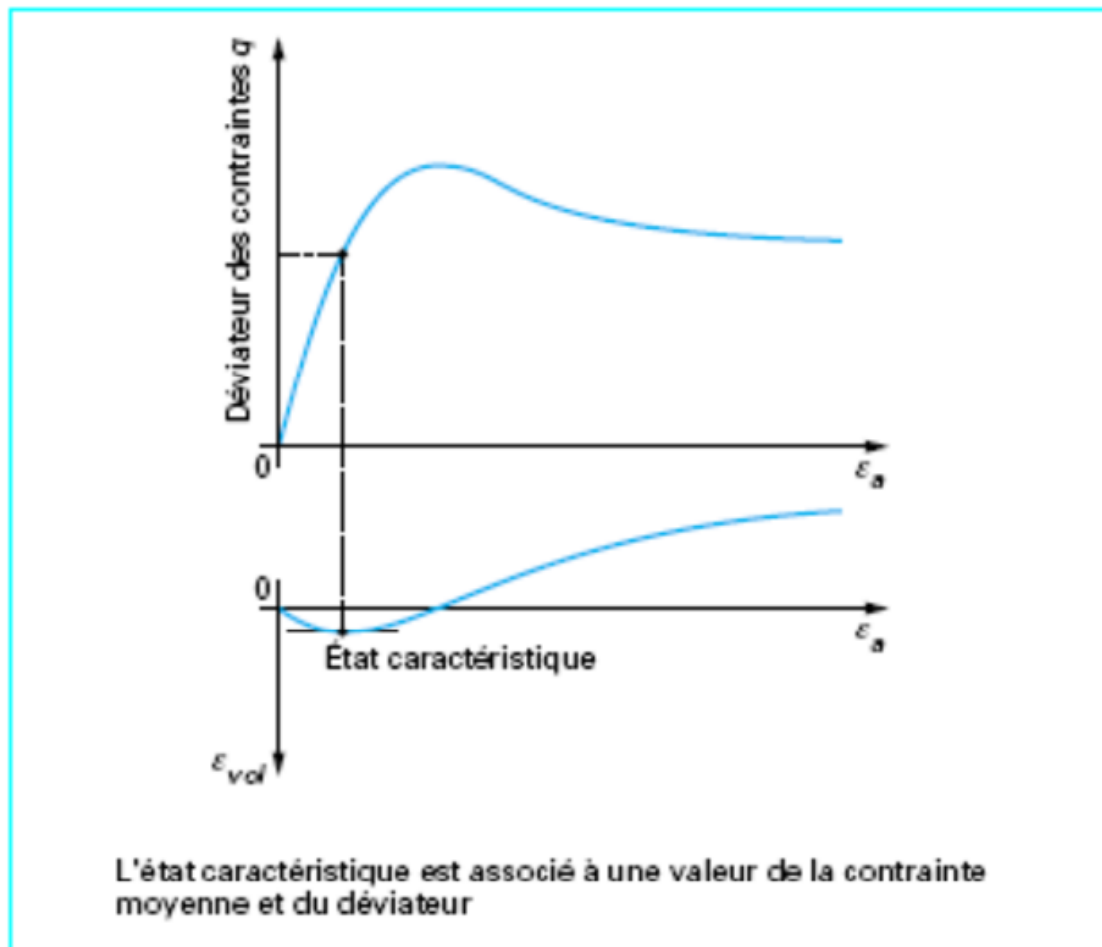


Figure 3.2: Definition of the Characteristic State



Figure 3.3: Earthquake aftermath and ground subsidence

Example: Dilative- Contractive Response in Triaxial Compression

Problem. Consider two dry sand specimens subjected to drained triaxial compression at the same initial mean effective stress p_0 :

- Specimen A: loose sand
- Specimen B: dense sand

Both specimens are sheared monotonically by increasing the axial stress σ_1 while the confining stress σ_3 remains constant.

1. Describe the expected volumetric behavior of each specimen.
2. Sketch qualitatively the evolution of volumetric strain ε_v with axial strain ε_1 .
3. Explain the link between dilatancy and shear strength.

Solution

1. Volumetric behavior

- **Loose sand (Specimen A):** The soil structure is open, and particles tend to rearrange into a denser configuration during shearing. As a result, the specimen exhibits *contractancy*, i.e., a decrease in volume ($\varepsilon_v < 0$).
- **Dense sand (Specimen B):** The particles are already tightly packed. During shear, grains must climb over one another, leading to an increase in volume. This behavior is known as *dilatancy* ($\varepsilon_v > 0$).

2. Volumetric strain response At small axial strains, both loose and dense sands may initially contract slightly. As shearing continues:

- Loose sand continues contracting until reaching a critical state.
- Dense sand reaches a minimum volume and then dilates progressively.

Qualitatively:

$$\varepsilon_v(\text{loose}) < 0 \quad \text{for all } \varepsilon_1, \quad \varepsilon_v(\text{dense}) : \text{contract} \rightarrow \text{dilate}$$

3. Relation to shear strength Dilatancy is directly linked to increased shear resistance. For dense sands, dilation causes an increase in mean effective stress, leading to a higher peak shear strength compared to the critical state strength. This behavior is commonly expressed using Rowe's stress–dilatancy relationship:

$$\frac{q}{p} = M + \frac{d\varepsilon_v}{d\varepsilon_s}, \quad (3.1)$$

where q is the deviatoric stress, p the mean stress, M the critical state stress ratio, and ε_s the shear strain.

Loose sands, being contractive, do not mobilize additional strength and therefore exhibit lower peak shear resistance.



4. Unsaturated Soil Behavior

4.1 Shrinkage and Swelling of Soils and Their Impact on Structures

4.1.1 Definition

Certain soils, especially clays, exhibit volume changes due to variations in moisture content:

1. Shrinkage: Reduction in soil volume when drying.
2. Swelling (Expansion): Increase in soil volume when wetting.
 - **Causes:** High plasticity clays absorb or lose water easily.
Seasonal fluctuations in groundwater level or rainfall.
Type and mineralogy of the clay (e.g., montmorillonite shows high swelling).
 - **Impact on Structures**
Differential settlements causing cracks in walls, floors, and foundations.
Damage to pavements and roads due to heaving or subsidence.
Tilting of lightweight structures built on expansive clays.
Damage to underground pipelines and utility lines from soil movement.
 - **Engineering Measures**
Moisture control around structures (drainage, landscaping).
Use of deep foundations or floating slabs to bypass active soil layers.
Soil stabilization with lime, cement, or geosynthetics.
Careful design of pavements and embankments to accommodate volume changes.

4.2 Definition of Suction

Suction in unsaturated soils refers to the **difference between pore air pressure and pore water pressure**, which generates an apparent cohesion and affects the mechanical and hydraulic behavior of soils. Suction controls **volume change, shear strength, and permeability** in partially saturated soils.

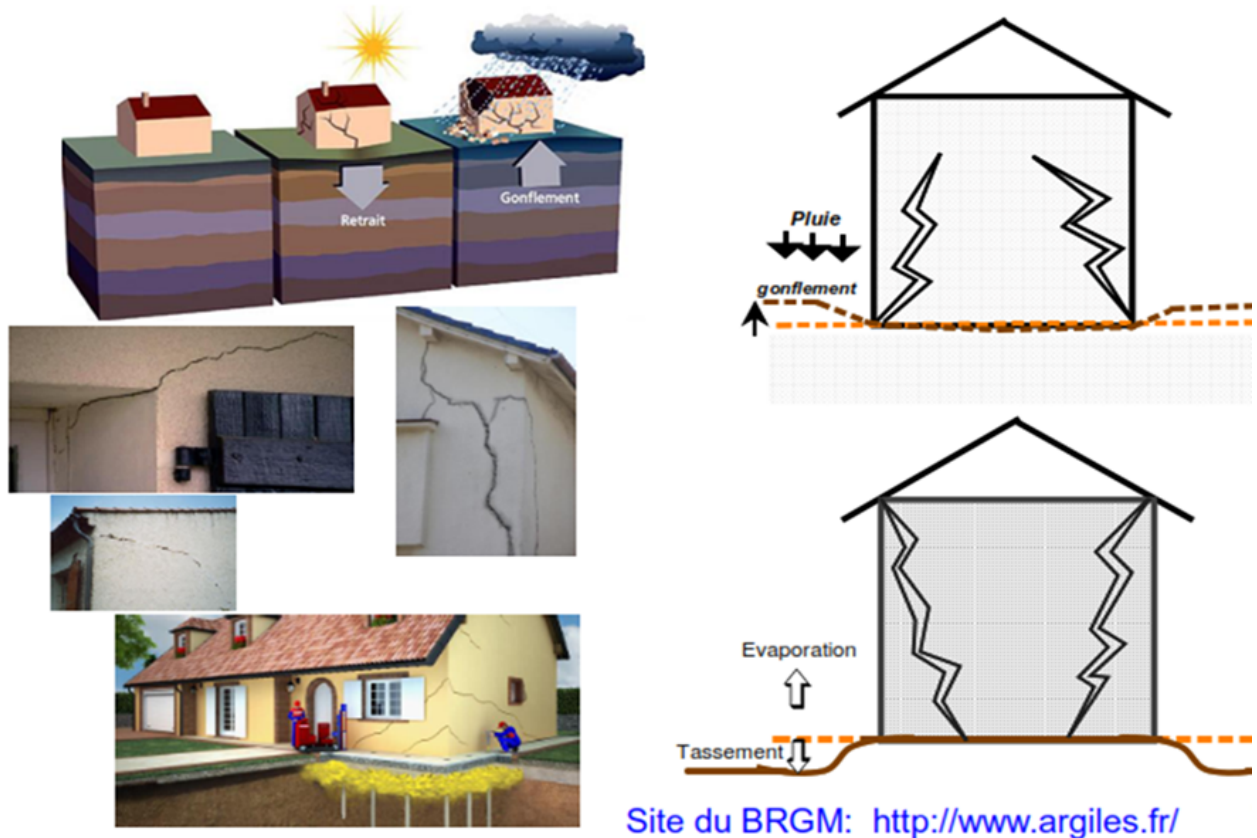


Figure 4.1: Shrinkage and Swelling of Soils and Their Impact on Structures

4.2.1 Concept of Effective Stress in Unsaturated Soils

In unsaturated soils, the classical Terzaghi effective stress principle is extended to account for **both air and water pressures**. The **effective stress** can be expressed as:

$$\sigma' = \sigma - u_a + \chi(u_a - u_w)$$

where σ is total stress, u_a is pore air pressure, u_w is pore water pressure, and χ is a parameter depending on degree of saturation. This concept is essential for evaluating **shear strength, deformation, and settlement** of unsaturated soils.

4.3 Water in Unsaturated Soils

Unsaturated soils are soils in which the **pores are partially filled with water and partially with air**. The behavior of water in these soils strongly affects the **mechanical, hydraulic, and chemical properties**. Understanding water distribution and movement is essential for **foundations, slopes, embankments, and environmental engineering**.

4.3.1 Soil Water Components

- **Gravitational Water:** Water that drains freely under gravity; not available to plants.
- **Capillary Water:** Water held in small pores by surface tension; important for soil strength and plant use.
- **Adsorbed Water (Hygroscopic Water):** Water tightly bound to soil particles; unavailable for plants but affects shrink-swell behavior.

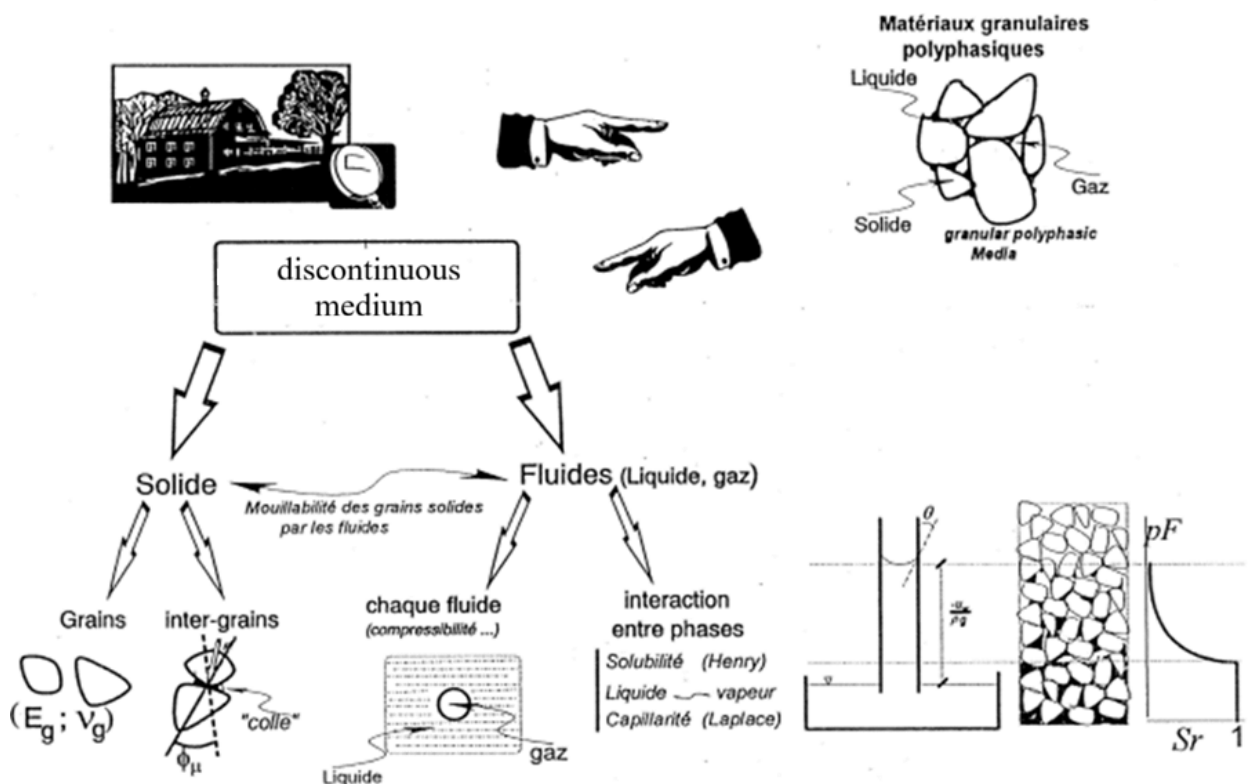


Figure 4.2: Concept of Effective Stress in Unsaturated Soils

4.3.2 Soil Moisture Characteristics

The **soil water retention curve (SWRC)** or **moisture characteristic curve** describes the relationship between **soil suction** (ψ) and **degree of saturation** (S_r) or **water content** (θ). Suction influences:

- **Effective stress** in unsaturated soils
- **Shear strength**
- **Permeability**
- **Volume change** (shrinkage and swelling)

4.3.3 Movement of Water in Unsaturated Soils

Water flow is governed by **capillarity, suction gradients, and gravity**. The flow can be described by **Richards' equation**:

$$\frac{\partial \theta}{\partial t} = \nabla \cdot [K(\theta) \nabla (\psi + z)]$$

where:

- θ = volumetric water content
- $K(\theta)$ = unsaturated hydraulic conductivity
- ψ = matric suction
- z = elevation head

4.3.4 Engineering Implications

- **Shear strength:** increases with suction due to apparent cohesion.
- **Settlement and volume changes:** influenced by drying/wetting cycles.

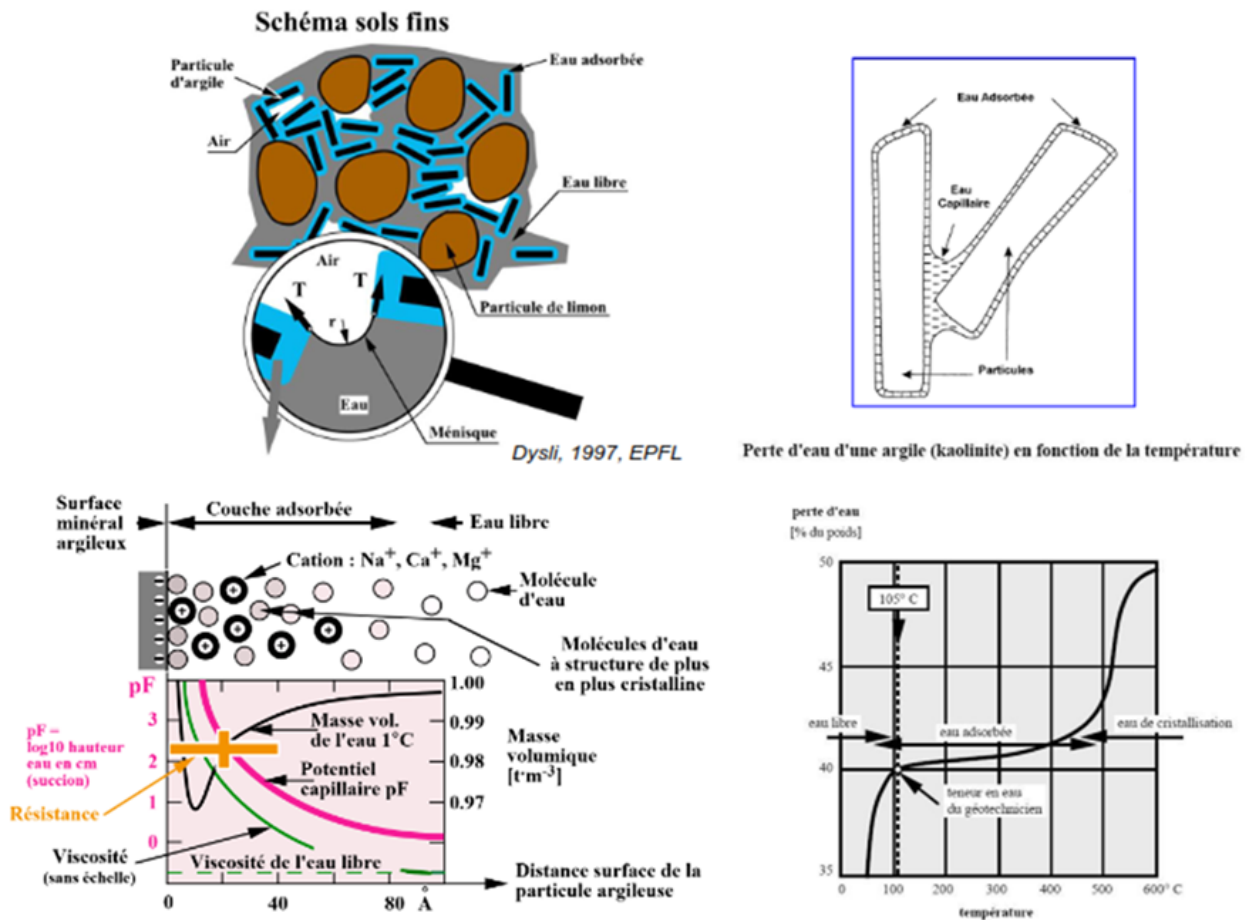


Figure 4.3: Water in Unsaturated Soils

- **Slope stability:** reduction in suction (e.g., after heavy rainfall) can trigger failures.
- **Permeability and seepage:** water flow is non-linear and depends on degree of saturation.

4.3.5 Shear Strength of Unsaturated Soils

Unsaturated soils exhibit higher shear strength than saturated soils due to the effect of **suction**. The extended Mohr-Coulomb criterion for unsaturated soils is often written as:

$$\tau = c' + (\sigma - u_a) \tan \phi' + (u_a - u_w) \tan \phi_b$$

where c' is effective cohesion, ϕ' is effective friction angle, and ϕ_b is the angle reflecting suction contribution. Shear strength depends on **degree of saturation, suction, and stress path**.

4.3.6 Permeability and Suction

Permeability in unsaturated soils is **suction-dependent**, decreasing as suction increases because water flows only through the partially saturated pores. The relationship is often expressed using **relative permeability functions** $k_r(S_r)$ in **unsaturated flow analysis**:

$$k_{unsat} = k_{sat} \cdot k_r(S_r)$$

where k_{sat} is saturated permeability and S_r is degree of saturation. Understanding permeability-suction relationships is critical for **seepage, slope stability, and infiltration problems**.

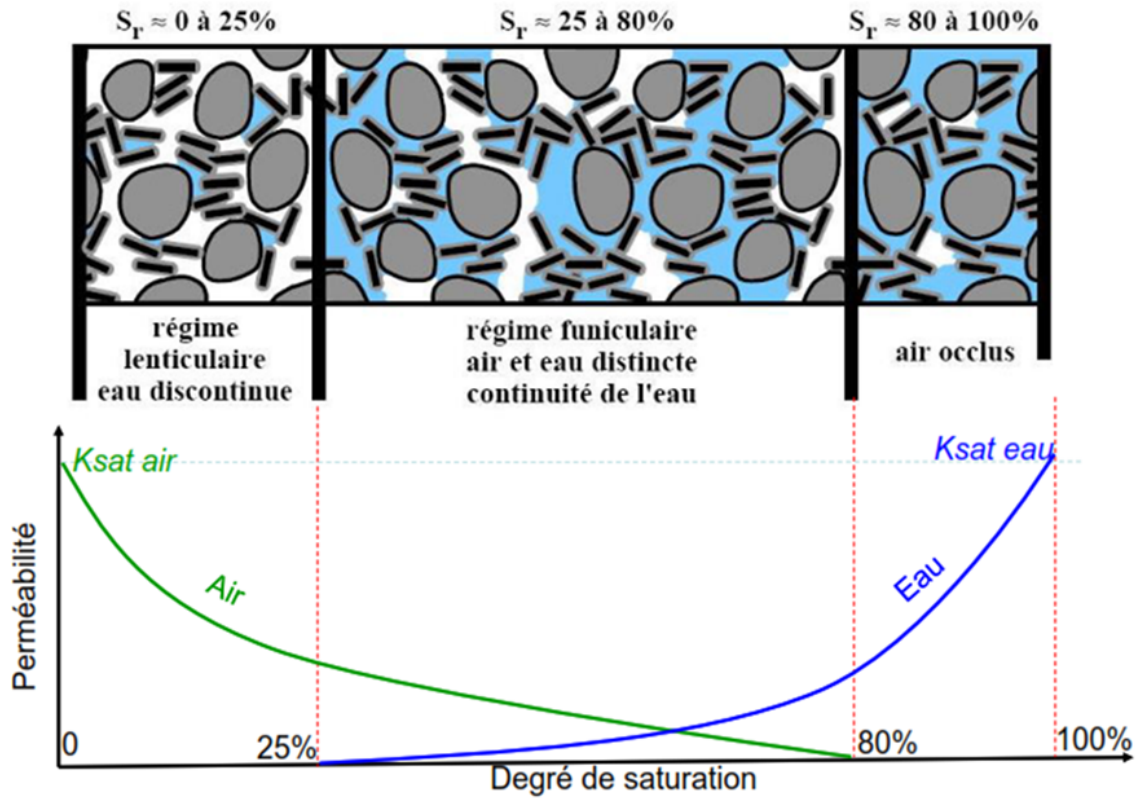


Figure 4.4: Permeability: Various Forms of Water in Unsaturated Soils

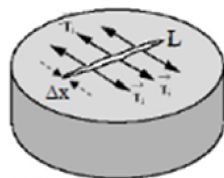
4.4 Properties of Water in an Unsaturated Porous Medium

4.4.1 Surface Tension Force

The phenomena previously observed are due to the existence of forces acting at the free surface of a liquid.

Let us imagine that we want to create, on the free surface of a liquid, an opening in the form of a slit of length L and very small width Δx . To do this, forces \vec{T}_i must be applied at several points along the edges of the opening. These forces must be **tractive forces**.

Indeed, the liquid tends to oppose this operation by developing a force \vec{F} of magnitude F that opposes the applied forces \vec{T}_i .



$$F = \gamma L$$



Thomas Schreyer

Figure 4.5: Analogy illustrating tensile forces: Forces acting on a slit created at the free surface of a liquid

The magnitude F of the force \vec{F} is proportional to the length L of the slit. Thus, we can write:

$$F = \gamma L$$

$$F = \gamma L$$

The coefficient γ is called the **surface tension** and is measured in Nm^{-1} .

The phenomena observed previously are due to the existence of forces at the **free surface of a liquid**. Consider creating a slit on the free surface of a liquid with **length** L and very small width Δx . To do this, forces T_i must be applied at several points along the slit, which act as **tensile forces**. Indeed, the liquid resists this operation by developing a force \mathbf{F} of magnitude F that opposes the applied forces T_i .

The magnitude F of the force \mathbf{F} is proportional to the length L of the slit. We can thus write:

$$F = \gamma \cdot L$$

The coefficient γ is called the **surface tension** and is measured in **N/m**.

4.4.2 Surface Tension and Pressure in a Bubble

Consider a liquid bubble of radius R that increases by a small increment dR .

Change in Surface Area:

$$\text{Surface area increase} = 4\pi(R + dR)^2 - 4\pi R^2 \approx 8\pi R dR$$

Work due to Surface Tension:

$$W_1 = \gamma \Delta A = \gamma \cdot 8\pi R dR$$

where γ is the surface tension.

Change in Volume:

$$\Delta V = \frac{4}{3}\pi(R + dR)^3 - \frac{4}{3}\pi R^3 \approx 4\pi R^2 dR$$

Work due to Pressure Increment:

$$W_2 = \Delta P \cdot \Delta V = \Delta P \cdot 4\pi R^2 dR$$

Equating the Works:

$$W_1 = W_2 \implies \Delta P = \frac{2\gamma}{R}$$

General Case (Non-Spherical Bubble):

$$\Delta P = \gamma \left(\frac{1}{R_1} + \frac{1}{R_2} \right)$$

where R_1 and R_2 are the principal radii of curvature of the bubble surface.

4.5 Measurement of Surface Tension

4.5.1 Capillary Method

By applying Jurin's law, the value of γ (surface tension) can be determined from the measurement of the capillary rise h and the knowledge of the other parameters.

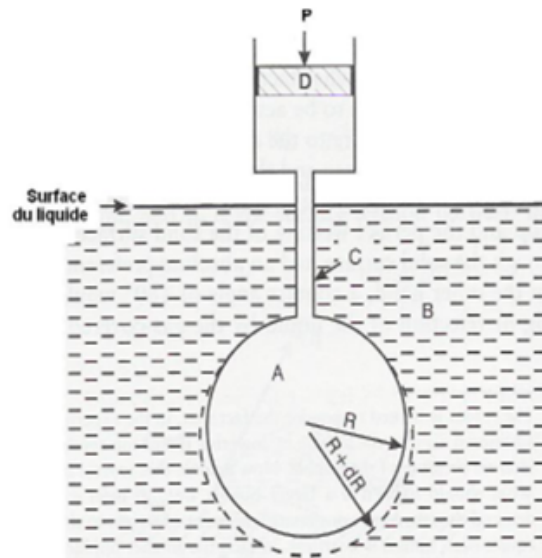


Figure 4.6: Surface Tension and Pressure in a Bubble

4.5.2 Tensile Force on a Submerged Plate

This refers to the force developed when a thin plate is pulled from a liquid, due to the surface tension at the liquid–air interface. The force is proportional to the perimeter of the plate in contact with the liquid. It is often used in experiments to measure surface tension, such as in the plate method (also called the Wilhelmy plate method).

$$F = \gamma P \quad (4.1)$$

where : F is the tensile force, γ is the surface tension, and P is the wet perimeter of the plate.

This method is widely used for precise measurements of surface tension in liquids. A metal plate of known mass is attached to one end of a balance beam. Once the beam is in equilibrium, with the plate positioned above the liquid, a container filled with the liquid is slowly raised using a screw mechanism. At the moment the plate contacts the liquid, an attractive force develops, and the plate is pulled into the liquid. To restore the beam to its equilibrium position, additional mass must be added to the opposite pan of the balance. The difference in mass between the two measurements allows the determination of the liquid's surface tension.

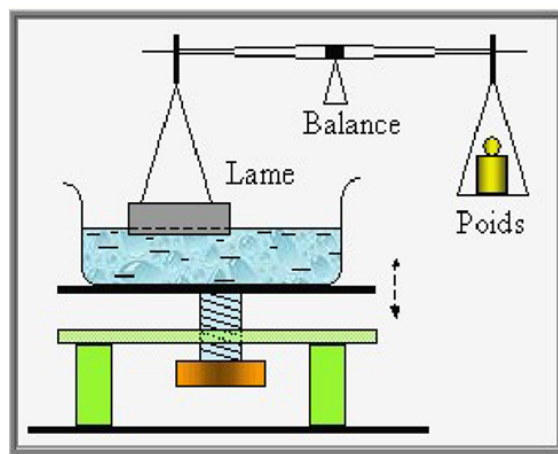


Figure 4.7: Tensile Force on a Submerged Plate

4.5.3 Wettability

4.5.4 Observations

When a liquid is placed on a solid surface, it may either spread out or form a droplet. The shape of the liquid at the interface is characterized by the contact angle (θ) between the liquid surface and the solid.

The angle θ is called the contact angle. It depends on the liquid, the solid supporting or containing it, and the gas surrounding both.

$\theta < 90^\circ$: The liquid wets the surface (spreads). $\theta > 90^\circ$: The liquid does not wet the surface (forms a droplet).

Contact angle directly affects capillary rise or depression in narrow tubes: Capillary rise occurs when the liquid wets the tube ($\theta < 90^\circ$).

Capillary depression occurs when the liquid does not wet the tube ($\theta > 90^\circ$). These phenomena are essential in understanding water movement in soils, thin films, and porous media.

- In a narrow glass tube (test tube), the air-liquid interface is curved downward: the surface forms a concave meniscus. Moreover, water rises along the walls.

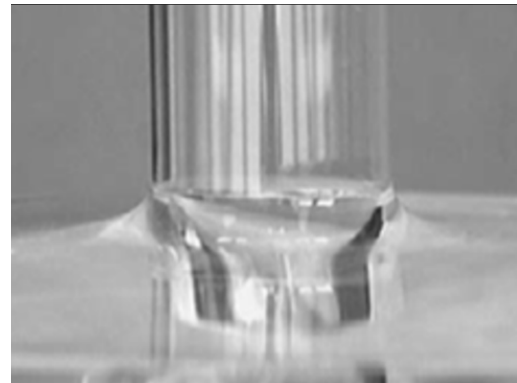


Figure 4.8: the air-liquid interface

- Water also rises along the fibers of a sheet of paper immersed in a glass of water. Therefore, capillary rise of water can occur despite gravitational forces.

4.5.5 Three Parameters Governing Contact Angle

The behavior of a liquid on a solid surface is governed by **three interfacial tensions**:

- **Solid–Liquid Interfacial Tension (γ_{sl})** – The surface energy between the solid and the liquid. It represents the tendency of the liquid to **adhere to the solid**.
- **Liquid–Vapor Surface Tension (γ_{lv})** – The surface tension of the liquid at the **interface with its vapor**. This is the classical **surface tension of the liquid**, which resists deformation and droplet spreading.
- **Solid–Vapor Surface Tension (γ_{sv})** – The surface energy between the solid and the surrounding gas. It reflects the solid's preference to be in contact with the vapor rather than the liquid.

These three tensions determine the **contact angle θ** through **Young's equation**:

$$\gamma_{sv} = \gamma_{sl} + \gamma_{lv} \cos \theta \quad (4.2)$$

- A drop of liquid deposited on a flat and horizontal solid surface may:

Understanding these parameters is essential for **capillarity, wetting phenomena, and water movement in soils**. (Example: water droplets on duck feathers coated with a greasy hydrophobic substance.)

- Spread out; in this case, the liquid is said to perfectly wet the solid.
- Form a lens-shaped drop, with two possible cases:
 - If $\theta < 90^\circ$, the liquid imperfectly wets the solid.(the liquid **wets** the solid surface.)
 - If $\theta > 90^\circ$, the liquid does not wet the solid.(the liquid **does not wet** the solid.)

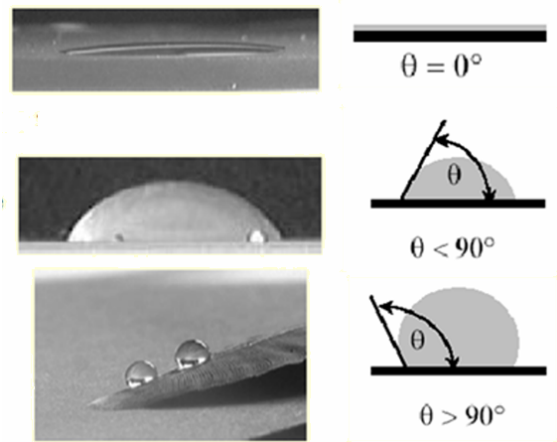


Figure 4.9: A drop of liquid

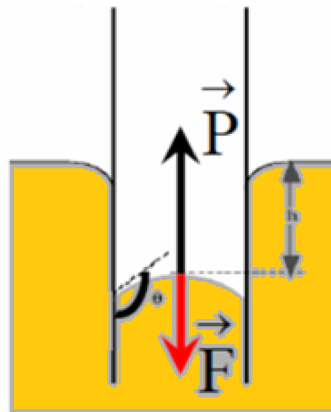


Figure 4.10

Remark

If the contact angle θ exceeds 90° , Jurin’s law gives a negative height h . This situation is referred to as **capillary depression**. It occurs in the case of mercury in contact with glass and for all non-wetting liquids.

In this case, cohesive forces are greater than adhesive forces, and the liquid does not wet the walls of the tube. The liquid level in the tube falls below the level of the free surface in the container. The meniscus is convex and forms an angle $\theta > 90^\circ$ with the tube wall.

Surface tension forces pull the liquid downward. The resultant of these forces balances the weight P of the missing liquid.

Table 4.1: Contact angle values for different glass interfaces

Interface in air	Contact angle θ ($^\circ$)	Capillary rise
Water – glass	0	↑
Organic liquid – glass	0	↑
Alcohol – glass	0	↑
Mercury – glass	140	↓

Table 4.2: Contact angle values for different interfaces

Interface in air	Contact angle θ ($^\circ$)	Capillary rise
Kerosene – glass	26	↑
Water – paraffin	107	↓
Water – steel	90	none
Water – wood	0	↑

Exercise: Nabil et al 2024

Objective: Study of the capillary rise phenomenon

Statement

1. Capillary rise in a tube

Consider a capillary tube with an internal diameter $d = 60\ \mu\text{m}$, immersed in a container filled with water, as shown in Figure(4.11). It is observed that the water rises inside the tube to a height h and forms a meniscus at the contact with air.

The surface tension is equal to $0.073\ \text{N m}^{-1}$ at a temperature $T = 20^\circ\text{C}$, and the contact angle between the meniscus and the wall of the tube is denoted by α .

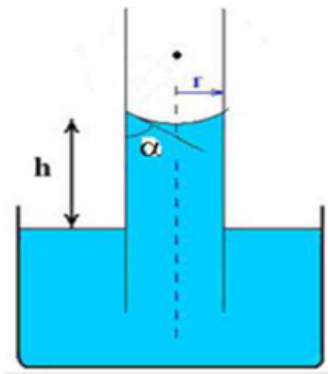


Figure 4.11: Representation of the capillary tub

- What are the suction and the pressure inside the water meniscus, in kPa , assuming that $\alpha = 0^\circ$?
- What is the height h of the water in the capillary tube?
- What does this height become if the contact angle is $\alpha = 45^\circ$?

2. Effect of the tube diameter

Repeat questions 1(a), (b), and (c) if the internal diameter of the capillary tube is $d = 1\ \mu\text{m}$.

3. Application to unsaturated soils *in situ*

Consider a soil layer exhibiting three different saturation zones:

a saturated zone (below the water table) and a zone saturated by capillarity of height h_c above the water table. This zone is overlain by an unsaturated zone, as shown in Figure 4.12.

3.1

Assume that the soil is a silt and that the average pore diameter is $d = 60\ \mu\text{m}$, the contact angle between the menisci and the soil grains is $\alpha = 30^\circ$, and the temperature is $T = 20^\circ\text{C}$.

- What are the suction and the pressure inside the water meniscus, in kPa ?

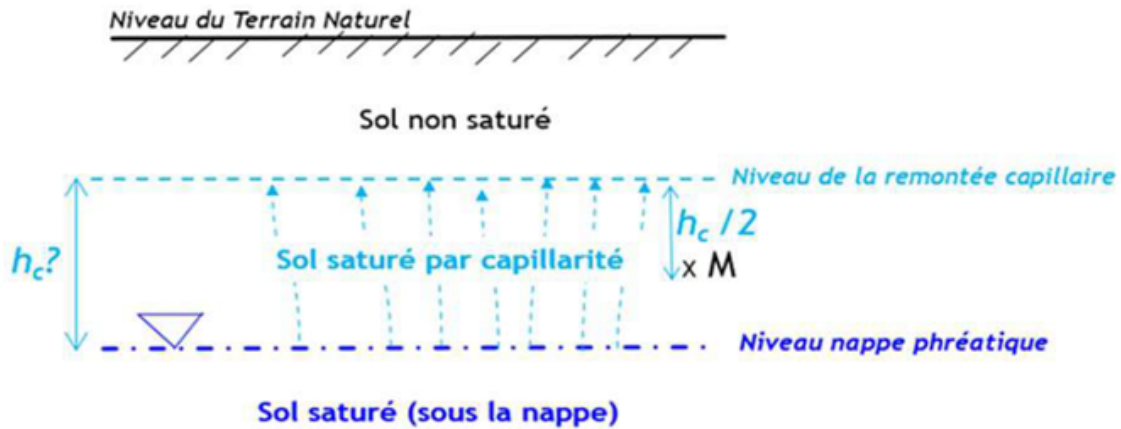


Figure 4.12: Representation of the capillary tub

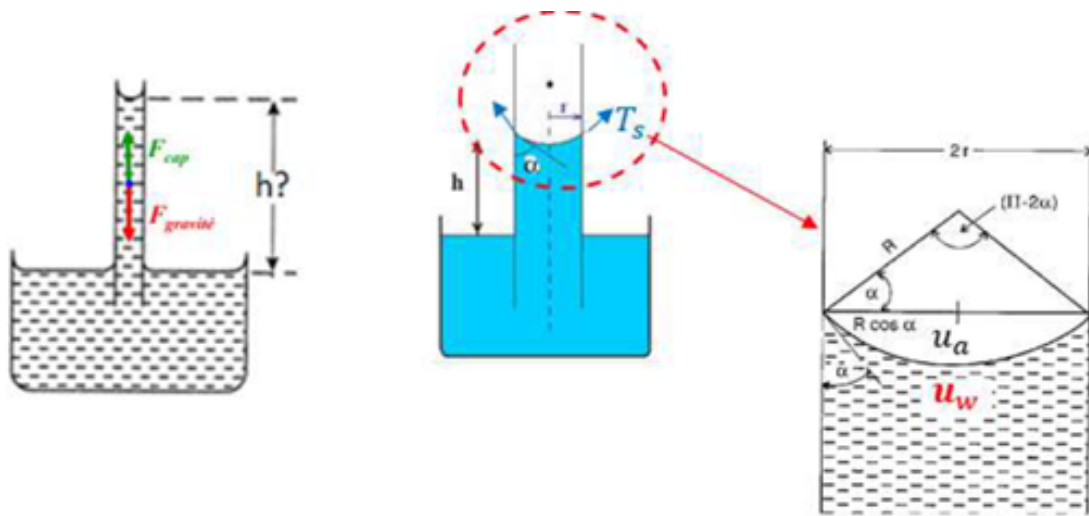


Figure 4.13: Representation of the parameters of Laplace's law

- b) Over what thickness (h_c) will this soil layer remain saturated by capillarity above the ground-water table?
- c) What is the value of the suction at point M located at $(h_c/2)$ in this case?

3.2

Assume that the soil is a clay and that the average pore diameter is $d = 1 \mu\text{m}$. Repeat questions 3.1 (a), (b), and (c).

3.3

During the summer period, the temperature in some Algerian regions can reach $T = 50^\circ\text{C}$. What happens to the answers to questions 3.1 (a, b) and 3.2 (a, b)?

3.4

What conclusions can you draw?

b) Height of the water column h in the capillary tube

The water rises in the tube until equilibrium is reached between the capillary rise force F_{cap} and the action of gravity on the liquid F_{grav} , which corresponds to the weight of the water column of height

h (Figure VII.3).

By writing the equilibrium equation, we obtain:

$$F_{\text{cap}} - F_{\text{grav}} = 0 \quad \Longleftrightarrow \quad F_{\text{cap}} = F_{\text{grav}} \quad (2)$$

Capillary rise force F_{cap} The capillary force is given by:

$$F_{\text{cap}} = \Delta P S = \Delta P \pi r^2 = \frac{2T_s \cos \alpha}{r} \pi r^2 = 2\pi r T_s \cos \alpha \quad (3)$$

Gravitational force F_{grav} The weight of the water in the tube is equal to the volume of water in the tube multiplied by the unit weight of water:

$$F_{\text{grav}} = \gamma_w V = \gamma_w \pi r^2 h \quad (4)$$

Expression of the capillary rise height Substituting equations (3) and (4) into equation (2), we obtain:

$$2\pi r T_s \cos \alpha = \gamma_w \pi r^2 h \quad \Longrightarrow \quad h = \frac{2T_s \cos \alpha}{\gamma_w r} \quad (5)$$

where:

$$T_s = 0.073 \text{ N/m}, \quad r = 30 \mu\text{m} = 30 \times 10^{-6} \text{ m}, \quad \gamma_w = 10 \text{ kN/m}^3 = 10^4 \text{ N/m}^3.$$

Numerical applications

Case $\alpha = 0^\circ$ Using equation (5):

$$h = \frac{2T_s \cos 0}{\gamma_w r} = \frac{2 \times 0.073}{10^4 \times 30 \times 10^{-6}} = 0.486 \text{ m} \approx 49 \text{ cm}.$$

Case $\alpha = 45^\circ$

$$h = \frac{2T_s \cos 45^\circ}{\gamma_w r} = \frac{2 \times 0.073 \times \cos 45^\circ}{10^4 \times 30 \times 10^{-6}} = 0.344 \text{ m} \approx 34 \text{ cm}.$$

2. Effect of the capillary tube diameter

Consider now a capillary tube with an internal diameter $d = 1 \mu\text{m}$ (i.e. $r = 0.5 \mu\text{m}$) and $\alpha = 0^\circ$.

a) Suction and pressure inside the meniscus

The suction is given by Laplace's law:

$$\Delta P = u_a - u_w = \frac{2T_s \cos \alpha}{r} = \frac{2 \times 0.073}{0.5 \times 10^{-6}} = 2.92 \times 10^5 \text{ N/m}^2 = 292 \text{ kPa}.$$

The pressure inside the meniscus is therefore:

$$u_w = u_a - 292 = 0 - 292 = -292 \text{ kPa}.$$

b) Height of water in the capillary tube

The capillary rise height is:

$$h = \frac{u_a - u_w}{\gamma_w} = \frac{292 \text{ kPa}}{10 \text{ kN/m}^3} = 29.2 \text{ m} \approx 30 \text{ m}.$$

c) Case $\alpha = 45^\circ$

$$h = \frac{2T_s \cos 45^\circ}{\gamma_w r} = \frac{2 \times 0.073 \times \cos 45^\circ}{10^4 \times 0.5 \times 10^{-6}} = 20.6 \text{ m} \approx 21 \text{ m}.$$

3. Application to unsaturated soils *in situ*

3.1 Silt soil

Assume that the soil is a **silt**, with an average pore diameter $d = 60 \mu\text{m}$ (i.e. $r = 30 \mu\text{m}$), a contact angle $\alpha = 30^\circ$, and a temperature $T = 20^\circ\text{C}$.

a) Suction and pressure inside the water meniscus

According to Laplace's law:

$$u_a - u_w = \frac{2T_s \cos \alpha}{r} = \frac{2 \times 0.073 \times \cos 30^\circ}{30 \times 10^{-6}} = 4.21 \times 10^3 \text{ N/m}^2 = 4.21 \text{ kPa.}$$

b) Thickness of the capillary-saturated zone

The thickness h_c of the soil layer saturated by capillarity above the groundwater table is:

$$h_c = \frac{u_a - u_w}{\gamma_w} = \frac{4.21 \text{ kPa}}{10 \text{ kN/m}^3} = 0.421 \text{ m} \approx 42 \text{ cm.}$$

c) Suction at point M located at $(h_c/2)$

At mid-height of the capillary zone:

$$u_a - u_w(M) = \frac{1}{2}(u_a - u_w) = \frac{4.21}{2} = 2.10 \text{ kPa.}$$

3.2 Clay soil

Assume now that the soil is a **clay**, with an average pore diameter $d = 1 \mu\text{m}$ (i.e. $r = 0.5 \mu\text{m}$).

a) Suction and pressure inside the water meniscus

$$u_a - u_w = \frac{2T_s \cos \alpha}{r} = \frac{2 \times 0.073 \times \cos 30^\circ}{0.5 \times 10^{-6}} = 253 \text{ kPa.}$$

b) Thickness of the capillary-saturated zone

$$h_c = \frac{u_a - u_w}{\gamma_w} = \frac{253 \text{ kPa}}{10 \text{ kN/m}^3} = 25.3 \text{ m.}$$

c) Suction at point M located at $(h_c/2)$

$$u_a - u_w(M) = \frac{1}{2} \times 253 = 126.5 \text{ kPa.}$$

3.3 Effect of temperature ($T = 50^\circ\text{C}$)

At higher temperature, the surface tension of water decreases. Consequently, the suction and the capillary rise height decrease proportionally.

Therefore, for both silt and clay soils:

- the suction $u_a - u_w$ decreases,
- the capillary rise height h_c decreases.

3.4 Conclusion

Capillary rise and suction:

- increase as the pore diameter decreases,
- decrease as the contact angle increases,
- decrease as the temperature increases.

Fine-grained soils (such as clays) can therefore sustain very high suctions and large capillary rise heights, whereas coarse-grained soils exhibit much smaller capillary effects.

References

1. Budhu, M., *Soil Mechanics and Foundations*
2. Das, B. M., *Principles of Geotechnical Engineering*, Cengage Learning.
3. Mitchell, J. K., & Soga, K., *Fundamentals of Soil Behavior*, 3rd Edition, Wiley.
4. Kramer, S. L., *Geotechnical Earthquake Engineering*, Prentice Hall.
5. Mitchell, J. K., & Soga, K., *Fundamentals of Soil Behavior*, 3rd Edition,
6. Fredlund, D. G., & Rahardjo, H., *Soil Mechanics for Unsaturated Soils*,
7. Terzaghi, K., Peck, R. B., & Mesri, G., *Soil Mechanics in Engineering Practice*,
8. Mitchell, J. K., & Soga, K., *Fundamentals of Soil Behavior*, 3rd Edition, Wiley.
9. Bagnold, R. A., *The Physics of Blown Sand and Desert Dunes*, Methuen, 1941.
10. Mécanique des sols non saturés Concepts de base et exercices corrigés Auteurs Nabil ABOU-BEKR et al Première Edition Novembre 2024